PHYSICAL CONTROLS ON SIERRA NEVADA TREELINE GROWTH AND IMPLICATIONS FOR CLIMATE RECONSTRUCTION

A Thesis submitted to the faculty of
San Francisco State University
In partial fulfillment of
the requirements for
the Degree

Master of Science

In

Geosciences

by

Lan Ma

San Francisco, California

May 2017

CERTIFICATION OF APPROVAL

I certify that I have read Physical Controls on Sierra Nevada Treeline Growth and Implications for Climate Reconstruction by Lan Ma, and that in my opinion this work meets the criteria for approving a thesis submitted in partial fulfillment of the requirement for the degree Master of Science in Geosciences at San Francisco State University.

Alexander Stine, Ph.D.
Assistant Professor

Petra Dekens, Ph.D.
Associate Professor

Kevin Simonin, Ph.D.
Assistant Professor

PHYSICAL CONTROLS OF SIERRA NEVADA TREELINE GROWTH AND IMPLICATIONS FOR CLIMATE RECONSTRUCTION

Lan Ma
San Francisco, California
2017

Tree-ring width (TRW) from the Sierra Nevada treeline has been widely sampled for reconstruction of past local temperature variability. We identified two challenges with the use of such records: (1) most collections from the region are decades-old, leaving a knowledge gap in tree growth response to recent climatic changes; (2) strong covariance between temperature and solar radiation permit ambiguity in attribution of growth response. We developed an updated TRW chronology using whitebark pine (*Pinus albicaulis*) from Sonora Pass, CA (38.32N, 119.64W; elev. 3130 m), which exhibits a strong correlation with May-Jun temperature ($r=0.36$, $p<0.001$). Moreover, an increasing correlation with previous winter (pOct-pNov) temperature in recent decades suggests the possibility of growth response shift due to climate warming. We also mapped all trees in the 80m x 70m study site to test for an influence of inter-tree shading on growth. We show that differences in growth rate between trees are predicted by competition ($r=-0.46$, $p<0.001$). We developed a directional competition index and show that competition effects on growth are strongly anisotropic and scale with average intensity of direct solar radiation, indicating that competition for incident radiation exists and light availability likely poses a control on growth at treeline environments.

I certify that the Abstract is a correct representation of the content of this thesis.

Chair, Thesis Committee

24 May 2017
Date

ACKNOWLEDGEMENTS

This research project could have been conducted without the help and support of numerous people. First I would like to thank my advisor, Dr. Zan Stine, for his resourcefulness, dedication, and demonstration of doing sound science; to my committee members, Dr. Petra Dekens, for her guidance on writing and valuable comments, and to Dr. Kevin Simonin, for his involvement to teach me plant physiology; and to Russell McArthur for his help with field work. This work is funded by the National Science Foundation.

In addition to academic support, I would also like to acknowledge my long-time friend, Dr. Andrew Friedman, and mentor, Dr. John Chiang, for their continued encouragement for me to pursuit graduate school.

Finally, I would like to express my profound gratitude to my family for their unconditional support through my years of study and research and for their understanding, or lack thereof, of why graduate school involves so much carpentry work! I would like to especially thank my dad for his assistance in the field and late night chats when I struggled to write. This accomplishment would not have been possible without them. Thank you.

TABLE OF CONTENTS

LIST OF FIGURES

Figures – CHAPTER 1 Page

Figures – CHAPTER 2 Page

CHAPTER 1

Suitability of Sonora Pass *Pinus albicaulis* for Climate Reconstruction

ABSTRACT

Tree-ring sampling for climate studies at Sierra treelines was conducted from the 1970s through the early 1990s and mostly restricted to the southern parts of the Central Sierra Nevada. While research in this area continues to be active, new sampling has been sparse. We investigate the suitability of using a northern Central Sierra treeline site to reconstruct past temperature and to produce an up-to-date chronology for the region to fill the gap on climate-growth relationships in the past 30 years. We developed a tree-ring width (TRW) chronology using whitebark pine (*Pinus albicaulis*) collected near Sonora Pass, CA. The chronology correlates most strongly with May-Jun temperature ($r = 0.39$, $p < 0.01$), indicating a potential for reconstructing early summer temperature. This timely chronology also reveals an increasing correlation with previous winter (pOct-pNov) temperatures in the recent three to four decades, suggesting the possibility of a growth response shift due to warming climates. Although the trees we sampled are relatively young (< 200 years-old) and thus not useful for climate reconstruction, we have identified much older (400-500 years-old) whitebark pine trees on similar elevations in the nearby area. The findings of this work justify for further field efforts to develop an early summer temperature reconstruction for the Central High Sierra.

1. INTRODUCTION

1.1. Tree-ring as a Climate Proxy

Given their widespread geographic coverage and high annual resolution, tree rings present a useful dating method to infer past environmental conditions. Generally, trees grow more and tend to yield wider rings during years of more favorable conditions, such as warm temperature or adequate water. Inversely, cold spells or droughts yield less growth and narrower rings. Additionally, large and small disturbances such as avalanche, fire, stand dynamics, or insects can also impact growth and leave scars on the rings. Tree growth is typically modeled using a complex set of variables (Eq. 1; Cook, 1985).

Equation 1: $R_t = f(A_t, C_t, D1_t, D2_t, E_t)$

Where R_t is the ring width for year t, A_t is the age-related growth trend, C_t is the climate-related growth trend and variations, $D1_t$ and $D2_t$ refer to endogenous and exogenous disturbance pulses, respectively, and E_t is other random variations. Of these, $\mathrm{D1_t}$ and $\mathrm{D2_t}$ are usually related to ecological events not covered in this study. Chapter 1 of this thesis focuses on the climate controls on growth ($\mathrm{C_t}$) after the removal of the age-related effects ($\mathrm{A_t}$). And Chapter 2 tackles on identifying an additional signal in what appears to be random noise ($\mathrm{E_t}$).

Climate control itself is expressed through multiple factors such as temperature, water availability, light availability, and nutrients. In order to single out the effects of any one climate signal on growth, tree-ring scientists focus on the most limiting environmental factor (limiting factor) on growth that controls the growth of an organism. For example, tree-ring records from arid climates such as the American Southwest are likely to respond to water availability, whereas records from cold climates such as the treeline ecotone are likely to covary with temperature. To reconstruct the variability of a climate variable, tree-ring scientists tend to focus on trees that grow in extreme environments where there is one factor that is most limiting on growth locally.

Climate reconstruction also requires the limiting factor to vary in intensity from year to year so that it is reflected as wide and narrow rings in the tree-ring record. These variations in ring width patterns allow for accurate cross-dating between multiple tree samples from one site. They also provide a sensitive chronology that respond temporally to inter-annual climate variabilities.

1.2. History of Temperature Reconstructions in the Central Sierra Nevada

The Central Sierra Nevada (CSN) is located in a Mediterranean climate band and varies considerably in elevation. This unique environment offers an ideal location for studying the impacts of multiple climatic factors on tree growth – the effect of water availability in a semi-arid zone and the effect of temperature in high-elevation treelines. Additionally, the presence of the sensitive and long-lived five-needle pines provides opportunities for paleoclimate reconstructions using tree-rings (Kipfmueller and Salzer, 2010). Since the 1970s and through more recent years, active climate-growth studies were conducted across this region (Lamarche, 1974; Peterson et al., 1990; Briffa et al., 1992; Brown et al., 1992; Graumlich, 1993; Scuderi, 1993; Millar et al., 2004; Bunn et al., 2005; Kipfmueller and Salzer, 2010, Dolanc et al., 2013).

These studies provided us with a foundational understanding of the temperature and precipitation variabilities over the past centuries and millennia in the Sierras. However, most of the core samples used in these studies were collected prior to the 1990s. Few ring-width records existed for calibration with instrumental measurements over the recent 30 or so years. This is also a period that observed some unprecedented climate extremes, most notably, record high global and local temperatures as well as severe droughts and floods. Other studies around the world show varying degrees of tree growth response – from the divergence problem where growth decreases despite warming temperatures (e.g. Briffa, 2004) to enhanced growth potentially attributed to increased carbon dioxide levels in the atmosphere. The lack of core samples from the CSN through the last 30 years leaves a knowledge gap on growth response to recent climate change in the Sierra Nevada. Furthermore, widespread tree mortality due to habitat shifts both regionally and globally (Larson, 2013) create a greater urgency to update existing chronologies or to resample from nearby areas to capture the growth response.

Most of the aforementioned studies also concentrated their sampling efforts near treeline of the eastern slopes in the southern parts of the CSN and the White Mountains, except for Dolanc et al., 2014, whose team sampled on the western slopes along major trans-Sierra highways and to as far north as South Lake Tahoe. Selecting a research site at Sonora Pass allows us to augment the existing studies and to evaluate whether tree growth responds differently across the CSN treeline ecotones.

The future climate of CSN is of high importance ecologically and sociologically. Not only is CSN home to abundant wildlife and vegetation, millions of Californians also rely on its snowpack as a source of drinking water. Each year, however, there is increasing anthropogenic stress to the CSN both as direct pollution deposited into the forests and as long-term, irreversible climatic shifts detrimental to the delicate environments.

Developing an up-to-date chronology provides a more recent comparison between tree-ring and instrumental records and deeper understanding of growth response in one of the most sensitive climate zones under a rapidly changing environment. Our first objective for this research is to expand the chronology collection both temporally (to include recent years up to 2014) and spatially (to include northern part of CSN at the divide between eastern and western slopes). Because most of the existing studies found both temperature and water availability signals in the tree ring record, we test whether tree growth near Sonora Pass exhibits similar responses. Our second objective is to evaluate the length and sensitivity of the chronology to determine the suitability of using Sonora Pass tree rings to reconstruct past climatic or ecological variabilities.

2. METHODS

2.1. Study Area

Our study area (Fig. 1; 38.32N, 119.64W, 3130m) is a treeline location along the Pacific Crest Trail near Sonora Pass, California. This 80m x 70m site sits on part of a relatively flat cirque bounded by sharp cliff drops on the west, north, and east sides, and by a peak of 3353 meters rising precipitously to the south. Multiple streams run around and through the site. The only tree species identified is whitebark pines (*Pinus albicaulis*), a common treeline species in the Sierra Nevada. It is visually apparent that trees in this region are increasingly stressed with elevation. Trees in our study area grow in tree-form but have a gnarred appearance, and they form small cluster patches across the site. Nearby trees located approximately 50 meters higher in elevation grow exclusively as isolated individuals or in krummholz form. Lower-elevation trees growing approximately 30 meters below the site are taller, thicker, and do not show the level of visual stress seen at the study site. These attributes of the site suggest that temperature variability is likely to play in important role in governing year-to-year variability in growth at our study location.

The climate of the Sonora Pass region is characterized by small seasonal temperature differences but a strong seasonality in precipitation (Fig. 2). Thirty-year climatology from nearby SNOTEL weather station #771 (38.32N, 119.60W, 2690m;

Supplemental Table S-1) indicates that annual temperature variability spans only about 17°C, with the highest temperatures occurring in July ($T_{avg} = 14°C$) and lowest from December through February ($T_{avg} = -3°C$). However, the diurnal temperatures can have approximately a 40°C range for almost all months of the year. Precipitation varies considerably throughout the year, ranging from an average of 14mm in August to 143mm in December. These coldest months align with the highest precipitation. Summer precipitation usually occurs as rain from convective storms. Given the temperature and precipitation range, the growing season at Sonora Pass area is approximately between June and September.

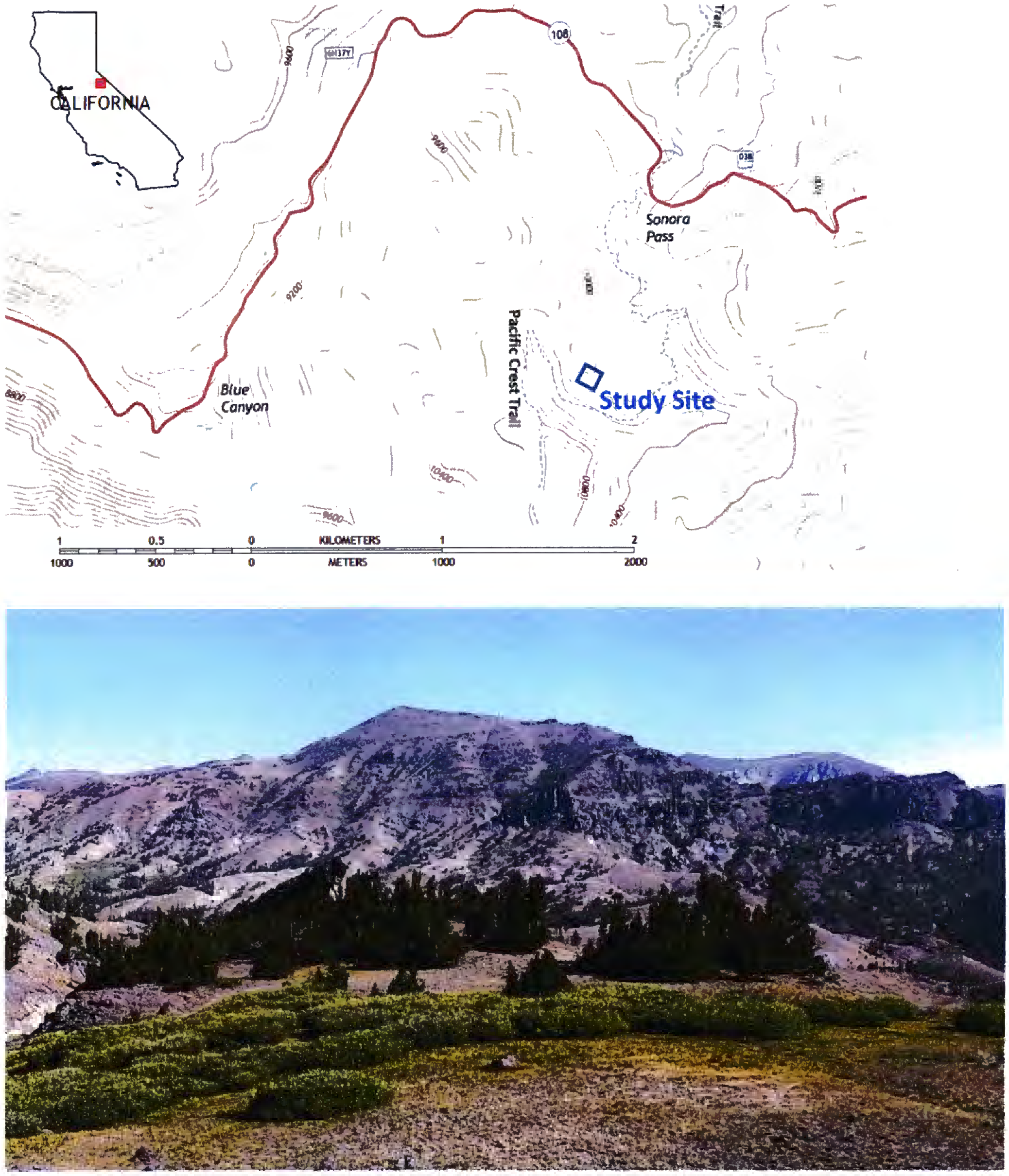

Figure 1. Site map and photo. (a) Topographic map of study site and region (elevation units in feet, with 80 ft. increments); inset map shows location of Sonora Pass in the Central Sierra Nevada range in California (USGS, 2015). **(b)** Photo of study site as viewed from Pacific Crest Trail looking north.

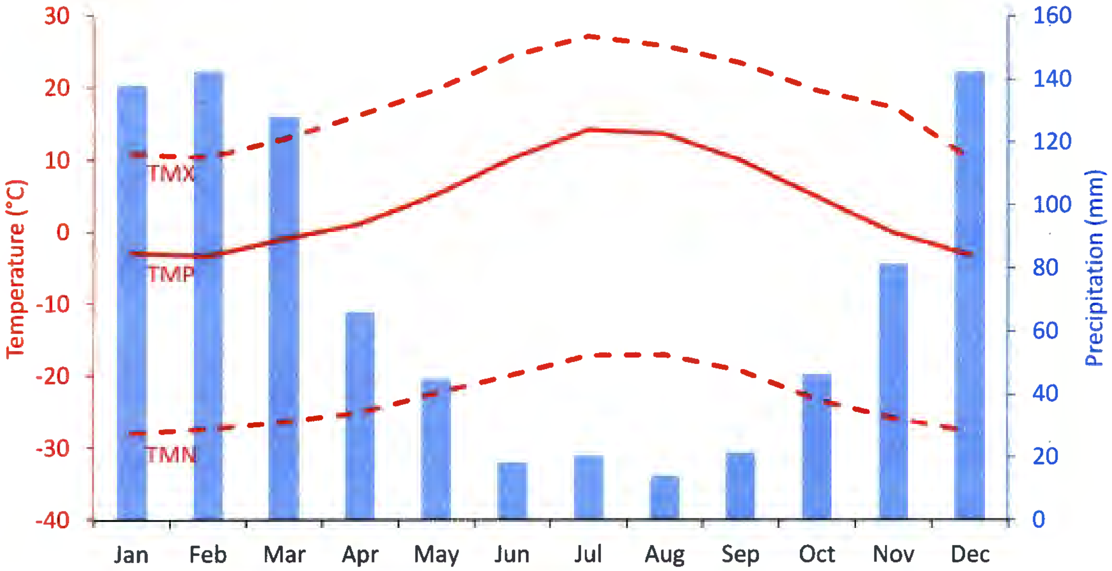

Figure 2. Temperature and precipitation climatology of Sonora Pass, CA. The monthly climatology represents 30-year averages between 1986 and 2015 from weather station SNOTEL 771 (38.32°, -119.60°, 2690m). Red lines represent monthly averaged maximum, mean, and minimum temperatures; blue bars represent monthly averaged precipitation.

2.2. Tree Core Sampling and Chronology Development

We sampled every tree having a diameter at breast height (DBH) greater than 12cm from the study site. Each tree was numbered, geo-located with a GPS unit (Garmin GPSmap 62stc), and cored using a 4.3-mm Haglöf increment borer. Depending on the size and accessibility of the trees, either one through-core or two radius cores were obtained per tree at breast height. For trees located on a slope, the cores were taken on the cross-slope sides of the trunk to avoid ring distortions due to the built structure. For trees with two or more branches, the branch with the larger DBH was sampled. We obtained 174 cores from 178 trees from the study site. In addition, we also collected 17 cores (13 trees) from the nearby area (within 0.5 km radius) to cross-date and to stabilize the chronology.

After core removal, we followed standard dendrochronology practices to process the samples in the laboratory (Stokes and Smiley, 1968). The cores were air-dried in their collection straws and then glued to a wood mount. We sanded cores at 400 and 600 grits using an electric belt sander and manually polished them with successively finer grits (up to 2500-grits) of sandpaper. They were visually cross-dated using skeleton plots (Fritts, 1976). Ring widths were measured on a Velmex linear micrometer stage with 0.001mm accuracy (Velmex Tree Ring Measuring System – TA) coupled with Tellervo (version 1.2.1) software. We used COFECHA to verify the skills of visual cross-dating (Holmes, 1983; Supplemental Table S-2). Only the cores that were confidently cross-dated were retained for chronology development. We standardized the series using ARSTAN program to distinguish the climate signal from the uneven age-related growth effects in the ring width series (Cook, 1985). We chose a two-step adaptive method to de-trend the series: negative exponential function was chosen as the default, but where the function fit went out of bound, a linear regression function was used (Holmes et al., 1986, Supplemental Table S-3). We also applied an auto-regressive model to remove persistence in the growth record and obtain the residual series (Holmes et al., 1986; Supplemental Table S-3). Lastly, we averaged the residual series using a bi-weight mean to enhance the common signal in the tree-ring width (TRW) chronology.

2.3. Climate Data and Correlations with TRW

There are four weather stations in the vicinity of the study site: SNOTEL site 711 and SRS, SRP, and DDM (Fig 3, Supplemental Table S-1). While we use information from these sites to derive seasonal patterns, they provide relatively short records (< 30 years). Instead, we used the Climate Research Unit high resolution (0.5° x 0.5°) TS v3.23 dataset, a grid-based product, to perform climate-growth correlation analysis. In particular, we obtained monthly temperature, precipitation, and cloud cover to test local climate controls on tree growth. We also removed the linear trends in both tree-ring width and climate time series to reduce correlation bias due to low frequency trends in the data. The correlations run from previous year October (end of previous growing season, denoted “pOct”) to current year September (end of current growing season) to capture the climate-growth relationship for the current growth year.

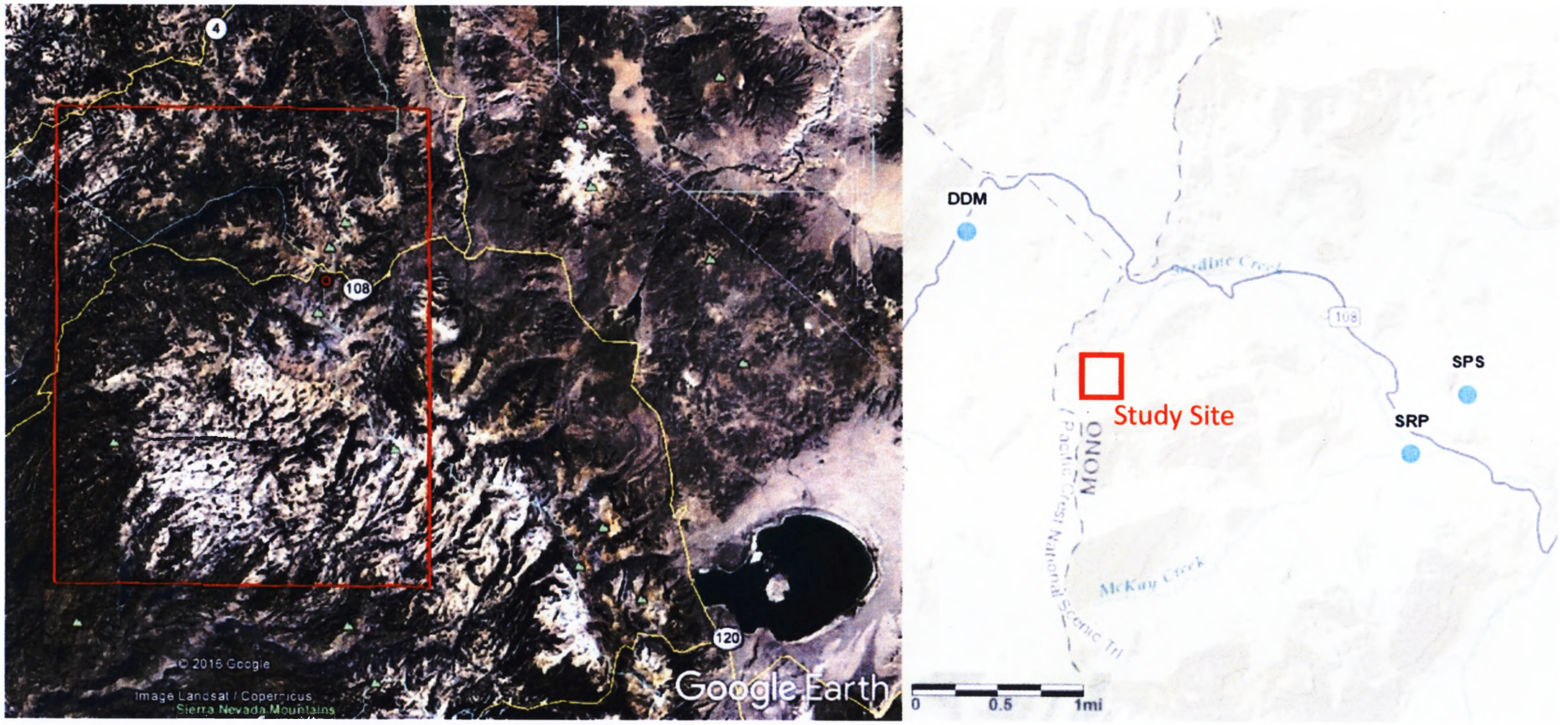

Fig 3. Climate data map. (a) CRU 0.5°x0.5° grid overlaid on Google Earth map; the red circle indicates the study site; **(b)** Locations of weather stations.

3 RESULTS

3.1 Ring-Width Chronology

Using 159 cores, we built a chronology that spans a relatively short period between 1814 and 2014, with an average age of 110 years (Fig 4a). Tree age is estimated by dating the most inner ring in the core samples. It does not represent the true age of a tree because it does not account for the years needed to reach breast height. However, because of the harsh environment at the altitude of this field site, we expect the time it takes for a tree to grow to breast height is not likely to vary significantly from tree to tree, and our estimates provide a relative establishment time for the area. The sample depth through time (Fig 4a, grey area) shows a gradual drop-off, indicating that trees in this area did not establish as a single cohort but rather in a continuous progression. Spatially, mixed stands of old and young trees grow across the field site (Fig 5), except for the lack of older trees (>100 years) on the northwest edge next to a cliff, suggesting establishment of trees did not follow a directional or elevations gradient across the study site.

Despite a relatively short record, our cores represent a stable and well-correlated chronology representing the temporal radial growth at a treeline environment near Sonora Pass. The averaged ring-width time series (Fig 4a, red line) is calculated as the ratio of the raw measurement to the standardized series and represented as a dimensionless index (Cook and Peters, 1997). The ring width index has a mean of one; positive departures from the mean indicate wider than average widths and negative departures refer to narrower than average widths. The variance of the chronology was adjusted by sample size (Fig 4a, grey histogram). This chronology has a mean inter-series correlation of 0.451, indicating that individual cores show moderate correlations with others in the chronology. The mean sensitivity of the chronology measures how sensitive the growth is to the year-to-year environmental variability. A value of 0.221 indicates a moderate response of the trees to environmental changes. The degree to which the cores collectively represent a coherent population climate signal in the chronology is calculated as the expressed population signal (EPS). EPS is a function of the number of samples for a given period and the mean series inter-correlation (Wigley et al. 1984). Over the 201-year chronology, the EPS is calculated for six 50-year windows and compared to an acceptable threshold of 0.85 (Wigley et al. 1984). The EPS for our chronology is consistently above this threshold, indicating the entire length of the chronology as a reliable indicator to a coherent population signal (Fig 4b).

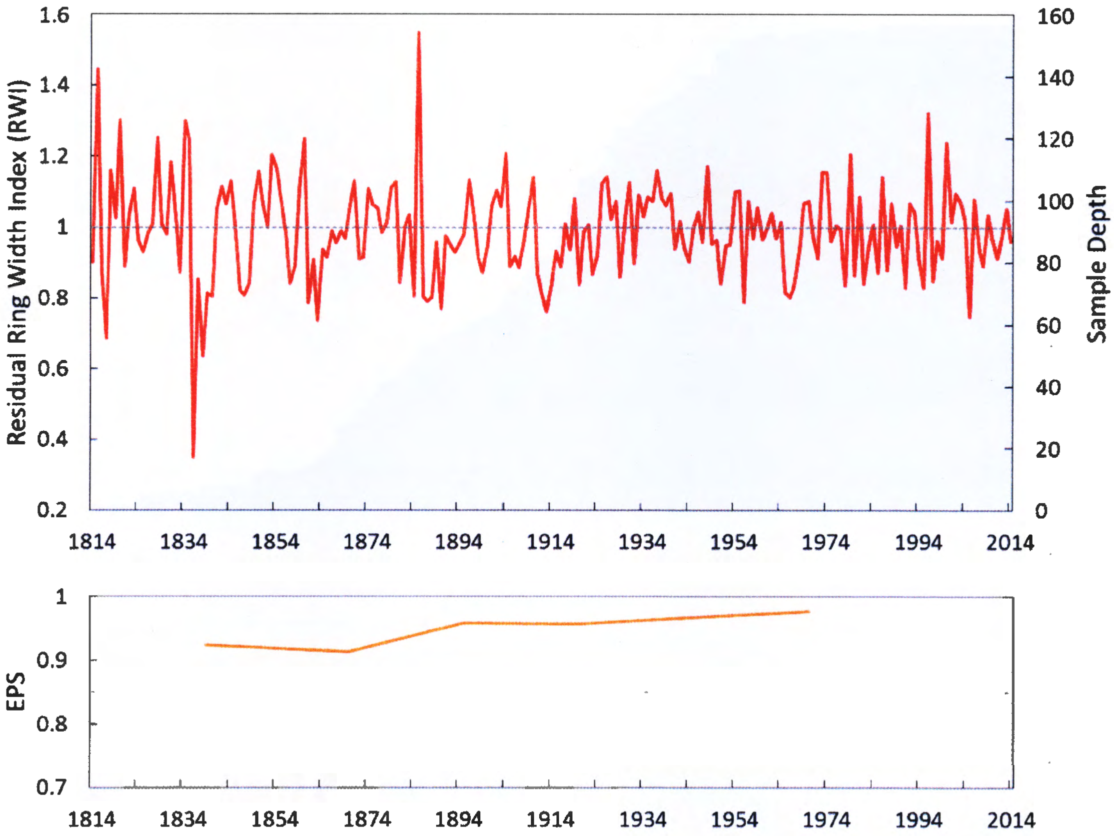

Figure 4. Ring-width chronology. (a) Averaged residual ring width chronology (red line); sample depth (grey shaded area), and **(b)** the 50-year running EPS (orange line) for the same time period.

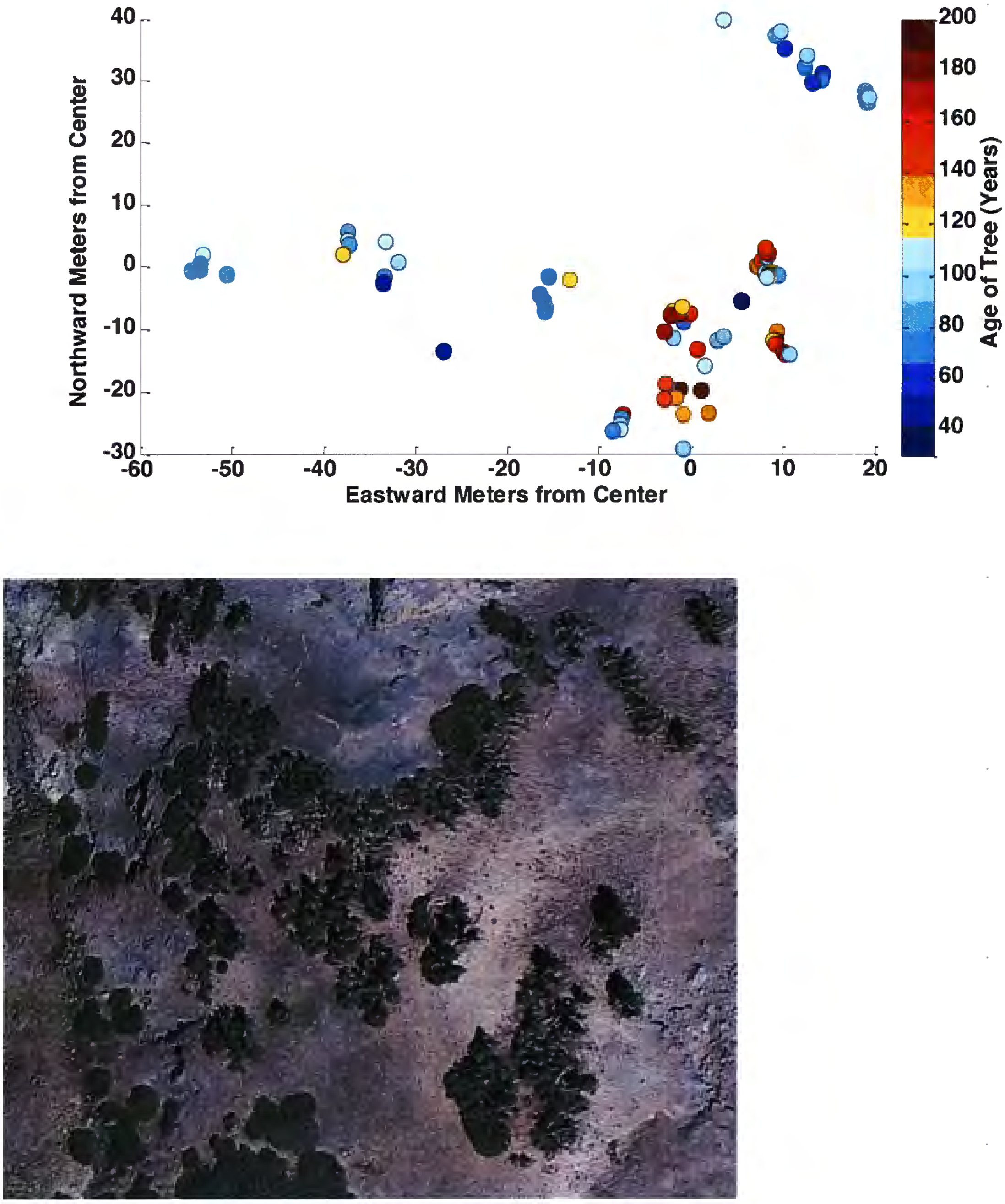

Figure 5. Spatial distribution of trees by age across the field site. (a) Relative locations of trees by age; **(b)** Arial photograph of site.

3.2 Positive Correlations with Temperature

Temperature is widely accepted as the primary control on growth in cold climates; we test whether or not that holds true in our Sierra treeline using Pearson product moment correlation between TRW and CRU monthly mean temperature. Ring width is positively and significantly correlated with May and Jun temperatures ($r_{may} = 0.23$, $p = 0.02$; $r_{jun} = 0.34$, $p < 0.001$, respectively, Fig 6). Together, May-Jun temperature variabilities explain about 13% of TRW variability during their overlapping period between 1901 and 2014 (Supplemental Fig S-1). Given the study site is often still under snow cover during May and sometimes into June, a warm early summer may signify an earlier start to the growing season. Also, the temperature-growth correlations from April to September are overall positive, though not all significant (Fig 6), which further supports the hypothesis that warm growing season temperature enhances growth. In general, strong correlations between ring width and spring-summer temperature are also consistent with a large body of evidence demonstrating temperature as a limiting factor on growth in treeline environments (LaMarche, 1974; Briffa et al., 1992; Bunn et al. 2005; Dolanc, 2013).

To a slightly smaller extent, the TRW chronology also correlates significantly with previous Oct ($r_{pOct} = 0.19$, $p = 0.04$) and Nov ($r_{pNov} = 0.22$; $p = 0.02$) temperature variabilities (Fig 6). Moreover, there is an overall positive relationship with winter temperature from pOct through Jan.

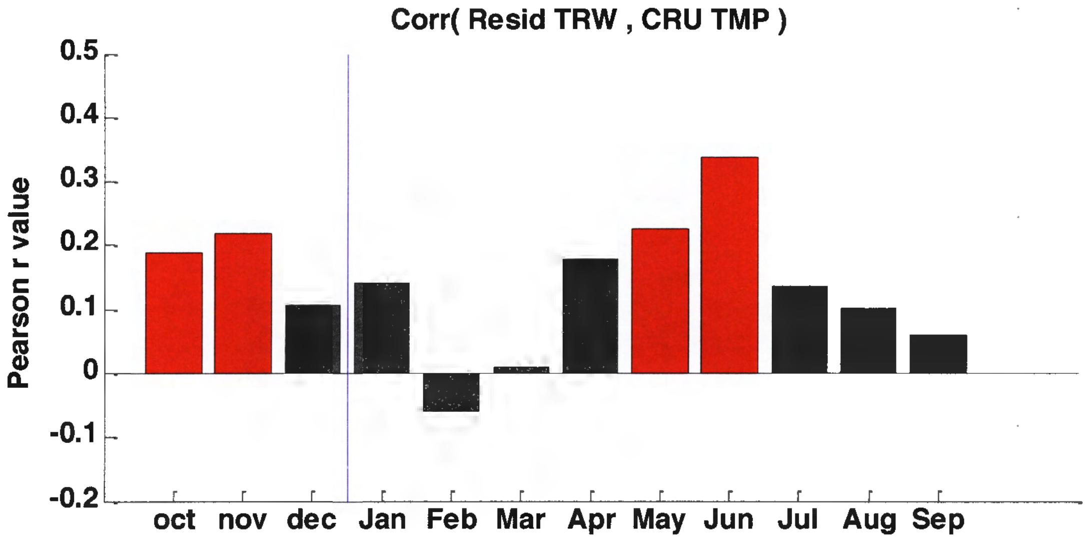

Figure 6. Pearson's correlation between TRW and temperature. CRU monthly average temperature runs from previous October (pOct) to current September (Sep). Significant correlations ($p < 0.05$) are highlighted in red.

Temperature limitation may occur in a relatively narrow band of elevations (Salzer, 2014), raising the concern that long-term variability in the vertical temperature profile may modulate the sensitivity of tree growth to seasonal temperature. To investigate this possibility, we calculate 30-year running correlations between temperature and tree growth (Fig 7). Results indicate that the temperature-growth relationship has not always been stable. Across the period of available data (1901-2014), spring-summer monthly (Apr through Jul) temperatures correlate well with the ring width record from the beginning of the century through about 1940. Thereafter, all of these correlations taper off, and only Jun correlation recovers to a significant level beginning in the early 1970s. Interestingly, the timing of this mid-century correlation drop is not unique. A growth response study found significant accelerated branch growth in six treeline sites in the Sierra Nevada during most of the 20th century, but branch growth was stable between 1945 and 1980 (Miller et al., 2004). Snowfield invasion by treeline trees had also accelerated significantly except for a decrease between 1950 and 1975 (Miller et al., 2004).

The correlations between previous late fall-winter temperatures and TRW also do not demonstrate temporal instability (Fig 7). In particular, correlations with pOct and pNov, which previously showed significant correlations (Fig 6), behave rather differently at higher frequency. pOct correlations start as weak at the beginning of the century, become negative and at times significantly negative between approximately 1940 and 1965, and become significantly positive from 1985 onward. TRW and pNov temperature are largely uncorrelated except for the initial 20 years and after 1995 which show significant and positively correlations. These observations suggest that the significant correlations for pOct and pNov through the entire 1901-2014 period (Fig 6) were largely weighed by high correlations at the end of the century or other low-frequency, century-scale, correlations. However, because the end-of-century correlation period is short (~ 30 years), it is difficult to conclude whether they can be explained by an ecological mechanism or they were a result of spurious statistics.

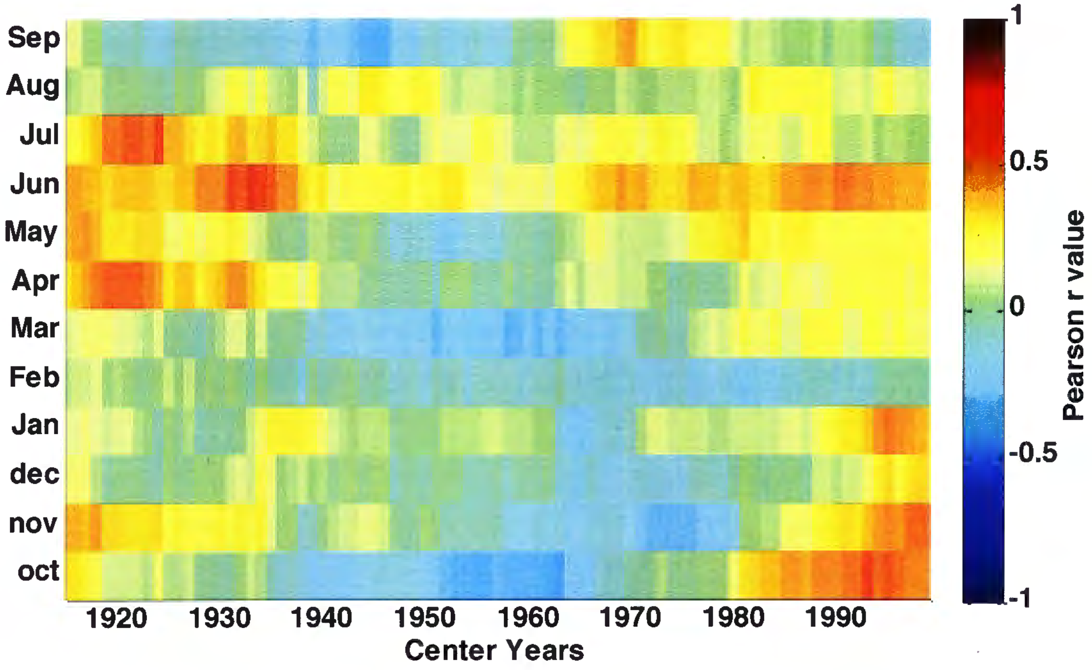

Figure 7. Moving correlations between TRW and CRU monthly temperature. Correlations calculated for 30-year windows between 1901 and 2014 (x-axis), and for each month from pOct to Sep (y-axis). Colors indicate magnitude of the correlations as Pearson's R.

3.3 Ambiguous Precipitation Signal

Water availability is of first order importance for tree growth at sub-treeline locations in the California Sierra (Stephenson, 1990). We investigate the possibility that water availability is also important at this treeline site using the CRU precipitation record. We find that the ring width record correlates strongly and positively with Feb precipitation ($r = 0.33$, $p < 0.001$, Fig 8). Distinct from temperature correlations, which spans a seasonal signal (Fig 6), correlation with Feb precipitation stands as a lone peak. Moreover, correlations with almost all months prior to and after February, though not all significant, point in the opposite direction, raising questions about its importance and significance. Moving correlations between Feb precipitation and TRW are stronger at the beginning of the century (prior to 1930) and only moderate but maintains positive throughout (Fig 9).

TRW also correlates negatively and significantly with Jun ($r = -0.19$, $p < 0.05$) and Aug ($r = -0.20$, $p = 0.03$) precipitation variabilities (Fig 8). Summer precipitation in this region is usually in the form of rain from convective storms, which can cause considerable cooling. Also, because TRW positively correlates with summer temperature (Fig 6), we hypothesize that the negative correlation with Jun and Aug precipitation is due to negative covariance between temperature and precipitation. To test this, we regressed the temperature variability out of the precipitation record and again compared residual precipitation to TRW. The resulting non-significant correlation between Jun and Aug precipitation supports this hypothesis.

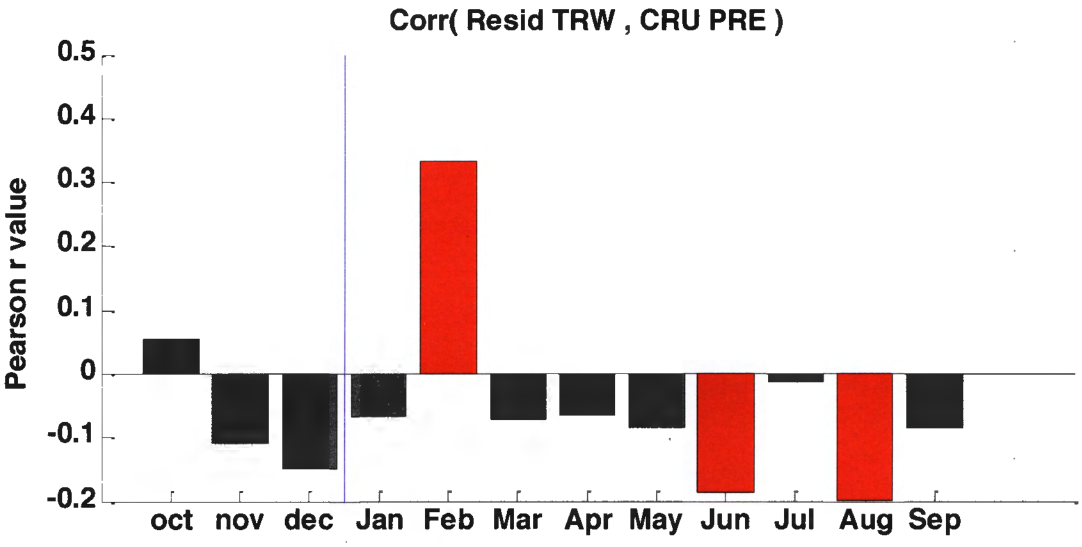

Figure 8. Correlation between TRW and monthly precipitation from pOct to Sep. Significant correlations ($p < 0.05$) are highlighted in red.

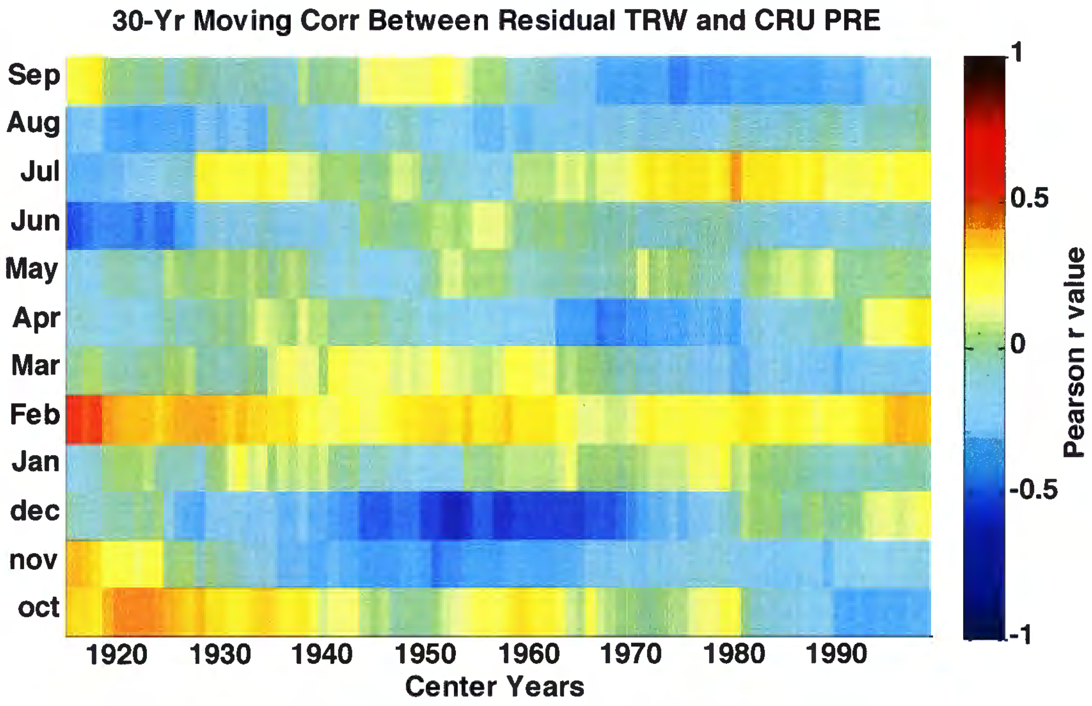

Figure 9. 30-year moving correlations between TRW and precipitation from pOct to Sep.

A surprising feature in the moving correlation analysis (Fig 9) is the significant, negative correlation between previous winter (pNov-pDec) precipitation and TRW for the period of 1940-1970. This is approximately the same mid-century timeframe when the May-Jun temperature correlation is weak (Fig 10). We further investigated the precipitation patterns from the CRU records. While there are large year-to-year variabilities in precipitation (most likely as snow in December) spanning the length of the instrumental record (Fig 11b), when precipitation is averaged over the same 30-year moving window as in the correlation analysis, this 1940-1970 period aligns with the some of the highest amounts of precipitation over the last century (Fig 11a). That is, during the few decades of high precipitation, more snowfall in previous December is correlated with less growth. This anomalously high winter precipitation period was recorded in other tree-ring reconstructions (Hughes and Brown, 1992; Graumlich, 1993), however, the sign of the correlation between precipitation and growth is inconsistent with other observations.

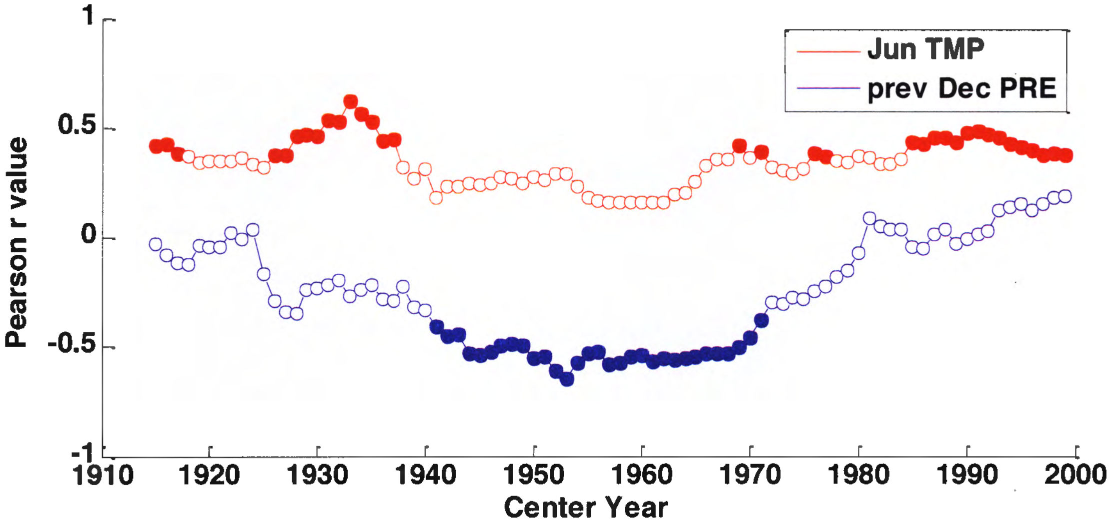

Fig 10. 30-year moving TRW correlations with Jun temperature (red) and pDec precipitation (blue). Significant correlations values ($p < 0.05$) are shown as closed circles.

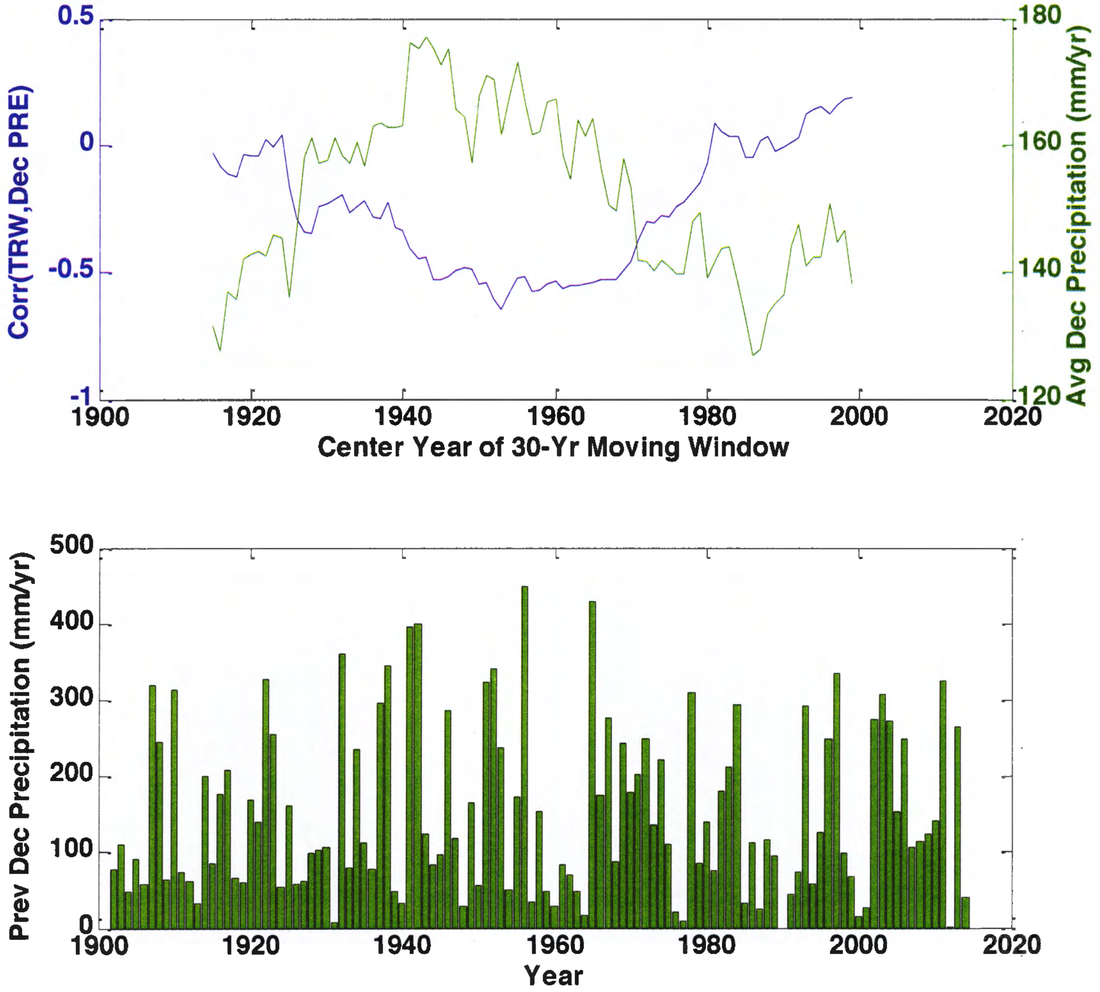

Fig 11. **(a)** 30-year moving correlation between ring width and previous December precipitation (blue) is most significant and negative when the 30-year running average of December precipitation was the highest over the last century. **(b)** Annual December precipitation shifted by one year to indicate the effect of previous year precipitation.

3.4 No Detection of Correlations with Light in Time Domain

Incident radiation promotes photosynthesis, motivating the test of large-scale light variability on tree growth in a treeline environment. Because there is no direct radiation records, we use negative cloud cover (NCL, absence of clouds) as a surrogate for light availability to explore its relationship with the TRW record. The patterns of the monthly correlations (Fig 12a), although largely insignificant, mimic those of the temperature correlations (Fig 6) – positive throughout the previous winter (pNov-Jan) and current late-spring and summer months (Apr-Sep), with significant correlations in June. This is not surprising because NCL and temperature strongly covary, and we suggest caution in interpreting correlations with NCL as an effect of light availability on growth. In general, less cloud cover yields more sunlight and leads to warmer temperatures. After regressing out temperature from the NCL record, the residual NCL shows no correlation with TRW (Fig 12b), indicating that correlation between TRW and NCL is largely tied to temperature variations.

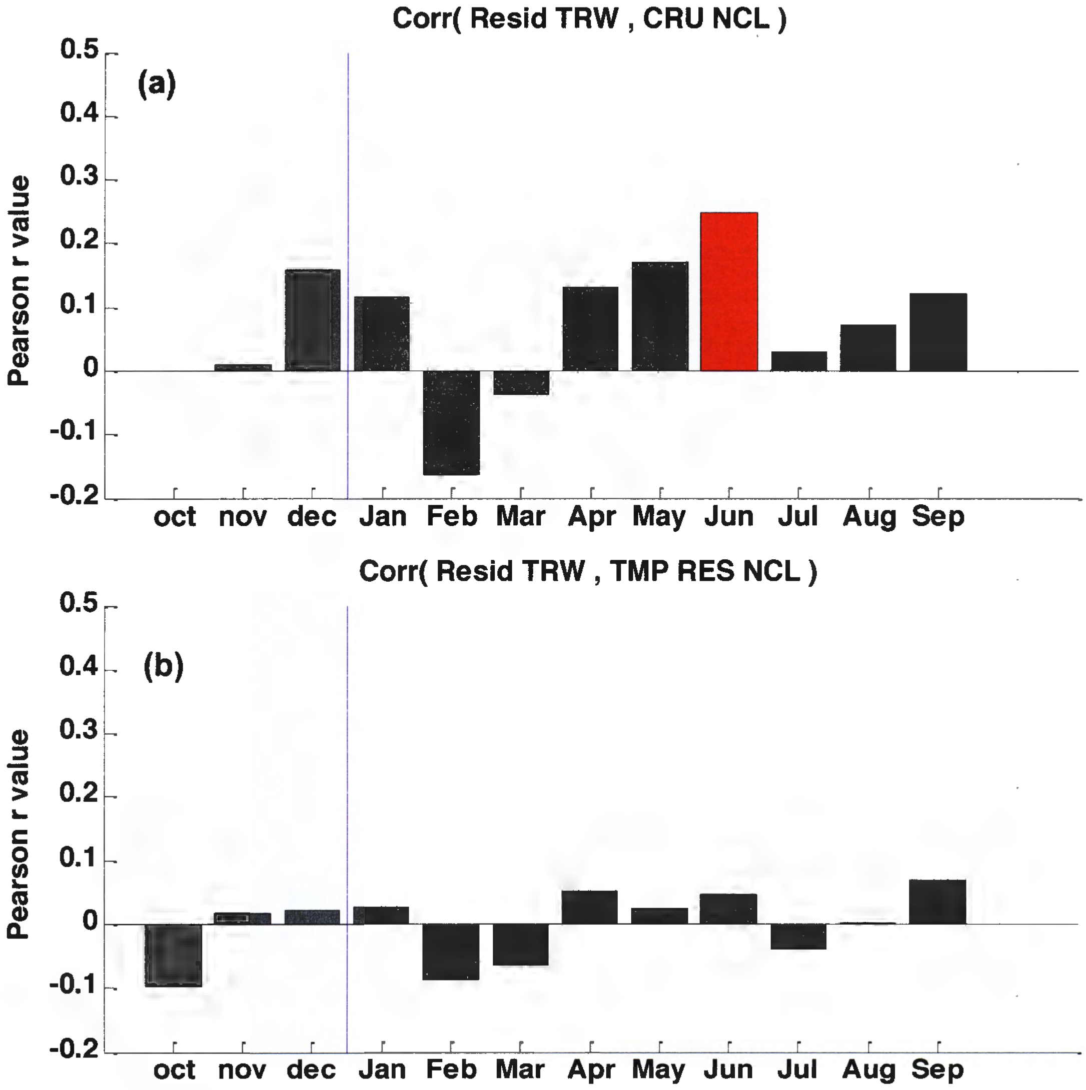

Figure 12. Relationships between TRW, light availability, and temperature. (a) Correlation between TRW and monthly negatively cloud cover (NCL) records from previous October to current September. (b) Correlations between TRW and temperature-regressed residual NCL. Significant correlations ($p < 0.05$) are highlighted in red.

4 DISCUSSION

4.1 Recent Collection Reveals Previous Winter TMP Correlations

The observation that previous late fall-winter (pOct-pNov) temperature becomes increasingly important on growth over the past three decades suggests a potential enhancement of carbon assimilation in warmer winters. pOct-pNov is a transition period marked by cool daytime temperature and freezing nighttime temperature. While radial growth may have ceased at this point, late-season warm daytime temperature may promote carbon assimilation, which results in carbon storage for the initial growth of the incoming year. Correlations with maximum temperature also show a stronger pOct-pNov signal than those with minimum temperature (Supplemental Fig S-3), suggesting that daytime temperature during this cool season can be a limiting factor to trigger photosynthesis. Warming over the recent decades may have resulted in late-fall and winter temperature just mild enough for carbon assimilation. The rise of correlation progressed gradually from fall (pOct, started around 1980) into winter (pNov-Jan), which fits in the physiological framework that warm days are more readily to occur in late-fall, and later into the winter period.

Another plausible explanation for the late-fall, early-winter correlations with growth is a result of climate memory. Results indicate that pOct-pNov temperatures are correlated with May-Jun temperatures ($r = 0.21$, $p < 0.03$).

Most of the tree-ring collections from the Central Sierra Nevada date back to the 1980s and early 1990s (ITRDB) and cannot be compared to instrumental climate records of the past 20-30 years. Our collection reveals an interesting, albeit short, rise in correlation between pOct-pNov temperature and TRW variabilities over the last three decades. If our observation is a result of ecological response, it suggests TRW will respond more strongly to previously late-fall, winter temperatures in a warming world. Because such correlations are not observed for most of the last century, our TRW records are unlikely to be useful for a pOct-pNov temperature reconstruction. However, the increasing influence of previous late-fall, early-winter temperatures on growth over the past three decades may override the correlation with early summer temperature in the near future, especially if this treeline area becomes less temperature limited due to global warming.

4.2 Possible Roles of Feb Precipitation on Growth

The strong and positive correlation with Feb precipitation - and not other months - suggest its potential direct and indirect roles on tree growth. Many Sierra Nevada tree-ring studies have reported positive correlations with previous winter precipitation spanning several months and have attributed its significance to moisture availability (Graumlich, 1991; Peterson, 1990; Bunn, 2005). However, the solo correlation peak with Feb precipitation is not unique to our site. Dolanc et al., 2013 also observed similar patterns for precipitation correlations on the western slopes of the Central Sierra Nevada but focused their interpretation using the Palmer Drought Severity Index (PDSI), which showed a positive seasonal correlation consistent with other findings.

4.3 Potential Interactions between TMP and PRE Controls on Growth

The stark alignment between the drop-off of the May-Jun temperature correlation during the mid-century period and rise of the pDec precipitation negative correlation (Fig 10) suggests the possibility of climate control regime shifts on tree growth in this region. For example, if temperature was particularly mild and precipitation was exceptionally low during this period, growth may become less temperature-sensitive but more moisture-limited. While low-frequency temperature has been on a steady rise over the past century, there is no indication of abnormal warmth between 1940 and 1970. Fig 11 also shows that precipitation during this period was the highest in the century. Both the sign of the pDec correlation and the relative amount of precipitation are inconsistent with the hypothesis of a drier climate shifting the growth control to precipitation.

Other possibilities for the lack of temperature correlation during the mid-century include endogenous and exogenous disturbances to the trees such as insects or fire, although such disturbances tend to occur in pulses and unlikely to last for three decades. On the other hand, a number of studies have reconstructed precipitation from high-frequency (annual to decadal scale) treeline TRW variabilities and reconstructed temperature from low-frequency (centennial scale) variabilities. Therefore 30-yr windows may not be an appropriate metric to capture the long-term temperature signal on growth.

4.4 Suitability of Climate Reconstruction

Understanding the frequencies at which these climatic factors are recorded in tree rings is also critical for reconstruction purposes. While some temporally unstable correlations exist, our TRW chronology moderately correlates with May-Jun instrumental temperature variabilities over a century-long overlapping period, making it a relatively reliable candidate for early summer temperature reconstruction at the low-frequency scale. For precipitation, however, the conflicting signs between correlations with pDec and Feb suggest complex interactions. Until we have a more established hypothesis to explain the correlations, we caution not to use our chronology to reconstruct past precipitation variabilities.

Our 200-year old chronology is relatively short for climate reconstruction. We originally chose this upper treeline environment in an attempt to maximize the temperature signal and a relatively flat site to minimize effects of uneven water distribution and ease of access. Topographically, the field site sits on a cirque. While it is more sheltered from fierce winds than on the ridge, it is more prone to rockslide events, which may have eliminated older trees. We have, however, identified other whitebark pines between 400 and 500 years old on a nearby (< 1km) but less accessible ridge. Our current study provides useful data and insights to evaluate the feasibility of sampling older trees for a longer temperature reconstruction.

5 CONCLUSION

The Central Sierra Nevada was subject to a large number of tree ring sampling and studies from the 1970s through the early 1990s. While research continues to be active, new sampling has been sparse. Our study provides not only an updated chronology for the region, the findings on increasing correlations with pOct-pNov temperature over the recent three decades also adds new understanding to tree-ring response to a period marked with unprecedented climate trends. The potential switch from summer to winter temperature limitation warrants continued research in this area to study treeline ecological response to a warming world.

Although our sampled trees are relatively young (< 200 years-old), we found a strong, positive correlation between TRW and May-Jun summer temperature, consistent with our hypothesis that growth at treeline environments are largely limited by temperature. Our chronology also correlates winter precipitation, but the conflicting signals between pDec and Feb correlations are problematic for reconstructions. Since we have identified much older (400-500 years-old) whitebark pine trees on similar elevations in the nearby area, our findings justify for further field efforts to sample the older trees to develop an early summer temperature reconstruction for the Central High Sierra.

6 REFERENCE

Briffa, K. R., P. D. Jones, and F. H. Schweingruber (1992), Tree-Ring Density Reconstructions of Summer Temperature Patterns across Western North America since 1600, *J. Climate*, *5*(7), 735–754, doi:10.1175/1520-0442(1992)005<0735:TRDROS>2.0.CO;2.

Briffa, K. R., T. J. Osborn, and F. H. Schweingruber (2004), Large-scale temperature inferences from tree rings: a review, *Global and Planetary Change*, *40*(1–2), 11–26, doi:10.1016/S0921-8181(03)00095-X.

Brown, P. M., M. K. Hughes, C. H. Baisan, T. W. Swetnam, and A. C. Caprio (1992), Giant Sequoia Ring-Width Chronologies from the Central Sierra Nevada, California, *Tree-Ring Bulletin.*

Bunn, A. G., L. J. Graumlich, and D. L. Urban (2005), Trends in twentieth-century tree growth at high elevations in the Sierra Nevada and White Mountains, USA, *The Holocene*, *15*(4), 481–488, doi:10.1191/0959683605hl827rp.

Cook, E. R. (1985), *A Time Series Analysis Approach to Tree-ring Standardization*, Tree-Ring Laboratory.

Cook, E. R., and K. Peters (1997), Calculating unbiased tree-ring indices for the study of climatic and environmental change, *The Holocene*, *7*(3), 361–370, doi:10.1177/095968369700700314.

Dolanc, C. R., R. D. Westfall, H. D. Safford, J. H. Thorne, and M. W. Schwartz (2013), Growth–climate relationships for six subalpine tree species in a Mediterranean climate, *Can. J. For. Res.*, *43*(12), 1114–1126, doi:10.1139/cjfr-2013-0196.

Fritts, H. C. (1976), Tree Rings and Climate, Academic Press.

Graumlich, L. J. (1993), A 1000-Year Record of Temperature and Precipitation in the Sierra Nevada, *Quaternary Research*, *39*(2), 249–255, doi:10.1006/qres.1993.1029.

Holmes, R. L. (1983) Computer-assisted quality control in tree -ring dating and measurement. Tree -Ring Bulletin 43: 69 -78.

Holmes, R. L., R. K. Adams, and H. C. Fritts (1986), Tree-Ring Chronologies of Western North America: California, Eastern Oregon and Northern Great Basin with Procedures Used in the Chronology Development Work Including Users Manuals for Computer Programs COFECHA and ARSTAN, *Laboratory of Tree-Ring Research Archives. The University of Arizona.*

Hughes, M. K., and P. M. Brown (1992), Drought frequency in central California since 101 B.C. recorded in giant sequoia tree rings, *Climate Dynamics*, *6*(3–4), 161–167, doi:10.1007/BF00193528.

Kipfmueller, K. F., and M. W. Salzer (2010), Linear trend and climate response of five-needle pines in the western United States related to treeline proximity, *Can. J. For. Res.*, *40*(1), 134–142, doi:10.1139/X09-187.

LaMarche, V. C. (1974), Paleoclimatic Inferences from Long Tree-Ring Records, *Science*, *183*(4129), 1043–1048, doi:10.1126/science.183.4129.1043.

Larson, E. R., S. Allen, N. L. Flinner, S. G. Labarge, and T. C. Wilding (2013), The Need and Means To Update Chronologies In A Dynamic Environment, *Tree-Ring Research*, *69*(1), 21–27, doi:10.3959/1536-1098-69.1.21.

Millar, C. I., R. D. Westfall, D. L. Delany, J. C. King, and L. J. Graumlich (2004), Response of Subalpine Conifers in the Sierra Nevada, California, U.S.A., to 20th-Century Warming and Decadal Climate Variability, *Arctic, Antarctic, and Alpine Research*, *36*(2), 181–200, doi:10.1657/1523-0430(2004)036[0181:ROSCIT]2.0.CO;2.

Peterson, D. L., M. J. Arbaugh, L. J. Robinson, and B. R. Derderian (1990), Growth Trends of Whitebark Pine and Lodgepole Pine in a Subalpine Sierra Nevada Forest, California, U.S.A., *Arctic and Alpine Research*, *22*(3), 233–243, doi:10.2307/1551586.

Salzer, M. W., E. R. Larson, A. G. Bunn, and M. K. Hughes (2014), Changing climate response in near-treeline bristlecone pine with elevation and aspect, *Environ. Res. Lett.*, *9*(11), 114007, doi:10.1088/1748-9326/9/11/114007.

Scuderi, L. A. (1993), A 2000-Year Tree Ring Record of Annual Temperatures in The Sierra Nevada Mountains, *Science*, *259*(5100), 1433–1436, doi:10.1126/science.259.5100.1433.

Stephenson, N. L. (1990). Climatic control of vegetation distribution: the role of the water balance. The American Naturalist, 135(5), 649-670.

Stockes, M. A., & Smiley, T. L. (1968). An Introduction to Tree-Ring Dating. Uni.

Wigley, T. M. L., K. R. Briffa, and P. D. Jones (1984), On the Average Value of Correlated Time Series, with Applications in Dendroclimatology and Hydrometeorology, *J. Climate Appl. Meteor.*, *23*(2), 201–213, doi:10.1175/1520-0450(1984)023<0201:OTAVOC>2.0.CO;2.

7 APPENDICES

7.1 Supplemental Tables

Table S-1. Climate data sources. Names of weather stations and dataset, climate variables measured, locations, and periods covered.

Station ID / Dataset	Station Name / Data Source	Latitude	Longitude	Elevation	Parameters	Periods	Operator
Weather Stations							
DDM	Deadman Creek	38.332°	-119.654°	2819m	TMP PRE SnowDC	2005-present 1987-present 1960-present	CA Dept. of Water Resources / Flood Management
SRP	Sonora Pass	38.313°	-119.607°	2667m	SnowDC	1930-present	Pacific Gas & Electric Company
SRS	Sonora Pass Bridge	38.318°	-119.601°	2667m	TMP PRE SnowDC	2005-present 1985-present 2004-present	Natural Resources Conservation Service
Site 771	Sonora Pass	38.317°	-119.600°	2690m	TMP PRE SnowDC SoilTM	1978-present 1978-present 1978-present 2004-present	National Water and Climate Center
Gridded Dataset							
TS v3.23	Climate Research Unit	0.5° x 0.5° grid		N/A	TMP PRE CLD PET VAP	1901-2014 1901-2014 1901-2014 1901-2014 1901-2014	University of East Anglia
N/A	Berkeley Earth	1° x 1° grid		N/A	TMP	1849-2015	Berkeley Earth

Parameter acronyms

TMP = Air temperature
PRE = Precipitation
CLD = Cloud cover
SDC = Snow depth and water content
VAP = Vapour pressure
PET = Potential Evapotranspiration
SoilTM = Soil temperature and moisture

Table S-2. Descriptive statistics of the chronology.

								//------------------ Unfiltered ------------------ -\\					//--------- Filtered ---------\\			
Seq	Series	Interval		No. Yrs	No. Segmt	No. Flags	Corr w/ Master	Mean msmt	Max msmt	Std dev	Auto corr	Mean sens	Max value	Std dev	Auto corr	AR
1	SP001J	1885	2014	130	5	0	0.441	0.56	1.3	0.193	0.603	0.217	2.74	0.413	-0.015	2
2	SP001K	1885	2014	130	5	1	0.389	0.69	1.53	0.244	0.572	0.234	2.67	0.441	0.001	2
3	SP002J	1824	2014	191	8	0	0.466	0.55	1.6	0.251	0.737	0.252	2.72	0.43	-0.05	1
4	SP002K	1824	2014	191	8	0	0.488	0.45	1.21	0.196	0.704	0.244	2.74	0.436	0.041	1
5	SP003A	1898	2014	117	5	2	0.4	0.93	2.22	0.446	0.822	0.219	2.61	0.429	-0.018	1
6	SP004J	1864	2014	151	6	1	0.477	0.63	1.43	0.227	0.644	0.238	2.57	0.359	-0.026	1
7	SP004K	1864	2014	151	6	1	0.43	0.59	1.45	0.208	0.606	0.233	2.62	0.443	0.06	1
8	SP007J	1868	2014	147	6	2	0.356	0.4	1.07	0.177	0.756	0.217	2.85	0.445	-0.025	3
9	SP007K	1868	2014	147	6	1	0.397	0.72	1.57	0.258	0.626	0.213	2.69	0.412	0.009	3
10	SP007Y	1872	2014	143	6	0	0.503	0.6	1.43	0.233	0.766	0.189	2.68	0.397	-0.072	1
11	SP007Z	1872	2014	143	6	0	0.434	0.47	1.02	0.149	0.625	0.198	2.61	0.305	-0.008	2
12	SP008J	1851	2014	164	6	2	0.385	0.33	0.68	0.114	0.674	0.234	2.63	0.414	-0.033	2
13	SP009K	1955	2014	60	2	0	0.438	0.4	0.76	0.137	0.738	0.198	2.61	0.446	0.007	1
14	SP011J	1985	2014	30	1	0	0.459	1.32	2	0.378	0.661	0.203	2.61	0.681	-0.065	1
15	SP011K	1985	2014	30	1	0	0.593	1.04	1.72	0.246	0.269	0.23	2.72	0.595	-0.078	1
16	SP016J	1877	2014	138	5	1	0.463	0.47	1.23	0.245	0.81	0.244	2.67	0.452	-0.058	1

								//---------------- Unfiltered ----------------- -\\					//--------- Filtered ---------\\			
Seq	Series	Interval		No. Yrs	No. Segmt	No. Flags	Corr w/ Master	Mean msmt	Max msmt	Std dev	Auto corr	Mean sens	Max value	Std dev	Auto corr	AR
17	SP016K	1877	2014	138	5	0	0.459	0.34	1	0.159	0.734	0.248	2.58	0.365	-0.036	1
18	SP017K	1876	2014	139	5	0	0.571	0.65	1.45	0.257	0.787	0.21	2.73	0.456	-0.024	1
19	SP019J	1875	2014	140	5	2	0.46	0.76	1.84	0.347	0.796	0.239	2.65	0.451	-0.046	1
20	SP019K	1875	2014	140	5	0	0.506	0.76	1.75	0.307	0.732	0.236	2.66	0.409	0.039	1
21	SP020J	1885	2014	130	5	0	0.556	0.71	1.34	0.221	0.741	0.186	2.68	0.492	0.041	1
22	SP020K	1885	2014	130	5	0	0.4	0.58	1.25	0.23	0.756	0.195	2.63	0.368	0.01	1
23	SP021J	1905	2014	110	4	0	0.485	0.36	0.86	0.155	0.765	0.227	2.78	0.532	-0.045	1
24	SP021K	1905	2014	110	4	0	0.601	0.38	0.83	0.151	0.732	0.239	2.68	0.454	-0.021	1
25	SP023J	1909	2014	106	4	0	0.551	0.89	1.77	0.274	0.583	0.22	2.71	0.429	0.049	2
26	SP023K	1909	2014	106	4	0	0.525	0.63	0.97	0.169	0.435	0.225	2.7	0.474	0.006	2
27	SP024A	1876	2014	139	5	0	0.564	1.22	3.19	0.475	0.716	0.193	2.92	0.393	0.022	1
28	SP024B	1918	2014	97	4	0	0.583	0.85	1.51	0.249	0.609	0.195	2.69	0.476	0.019	1
29	SP025J	1886	2014	129	5	0	0.561	0.33	0.99	0.173	0.86	0.194	2.57	0.413	-0.094	1
30	SP025K	1886	2014	129	5	0	0.387	0.37	1.41	0.317	0.929	0.239	2.67	0.396	-0.006	1
31	SP026J	1884	2014	131	5	2	0.397	0.35	0.84	0.158	0.629	0.267	2.83	0.5	-0.078	1
32	SP026K	1884	2014	131	5	1	0.377	0.65	1.79	0.346	0.844	0.226	2.83	0.438	0.009	1
33	SP029K	1895	2014	120	5	1	0.303	0.76	2.47	0.415	0.736	0.225	2.78	0.45	-0.04	1
34	SP030K	1907	2014	108	4	0	0.494	0.44	1.56	0.29	0.858	0.296	2.93	0.546	-0.045	2

								//------------------ Unfiltered -------------------\\					//--------- Filtered ---------\\			
Seq	Series	Interval		No. Yrs	No. Segmt	No. Flags	Corr w/ Master	Mean msmt	Max msmt	Std dev	Auto corr	Mean sens	Max value	Std dev	Auto corr	AR
35	SP032J	1896	2014	119	5	0	0.565	0.35	0.67	0.124	0.752	0.194	2.75	0.429	-0.008	2
36	SP032K	1896	2014	119	5	0	0.499	0.69	1.26	0.238	0.785	0.178	2.56	0.359	0.014	3
37	SP035J	1940	2014	75	3	2	0.367	0.83	1.37	0.218	0.647	0.175	2.65	0.501	0.034	1
38	SP035K	1940	2014	75	3	0	0.486	0.7	1.56	0.239	0.76	0.177	2.74	0.471	0.008	1
39	SP038J	1918	2014	97	4	3	0.387	0.48	0.88	0.163	0.707	0.203	2.69	0.589	0.093	1
40	SP038K	1918	2014	97	4	0	0.551	0.41	0.86	0.152	0.686	0.222	2.76	0.485	-0.018	1
41	SP039J	1916	2014	99	4	0	0.533	0.69	1.54	0.273	0.812	0.189	2.5	0.444	-0.039	1
42	SP039K	1916	2014	99	4	1	0.451	0.56	1.46	0.263	0.88	0.184	2.54	0.354	-0.053	1
43	SP040J	1915	2014	100	4	0	0.56	0.59	1.11	0.183	0.732	0.181	2.58	0.368	-0.049	1
44	SP040K	1915	2014	100	4	0	0.651	0.64	1.04	0.142	0.566	0.163	2.67	0.466	-0.066	1
45	SP041J	1874	2014	141	6	1	0.374	0.33	0.9	0.172	0.797	0.245	2.65	0.367	0.015	1
46	SP047J	1903	2014	112	4	1	0.341	0.67	1.63	0.306	0.831	0.201	2.64	0.326	-0.009	1
47	SP053J	1825	2014	190	7	0	0.497	0.41	1.46	0.249	0.842	0.259	2.91	0.479	-0.015	2
48	SP053K	1825	2014	190	7	3	0.357	0.56	1.34	0.251	0.847	0.189	2.62	0.388	-0.005	2
49	SP054J	1814	2014	201	8	0	0.586	0.46	1.06	0.198	0.77	0.229	3.06	0.441	0.03	1
50	SP054K	1814	2014	201	8	0	0.441	0.58	2.08	0.363	0.868	0.232	2.65	0.305	-0.055	1
51	SP054Y	1837	2014	178	7	2	0.379	0.68	1.79	0.314	0.833	0.2	2.63	0.32	-0.011	2
52	SP054Z	1837	2014	178	7	0	0.596	0.43	1.19	0.202	0.765	0.223	3.01	0.466	0.033	1

								//------------------- Unfiltered ------------------ -\\					//---------- Filtered ----------\\			
Seq	Series	Interval		No. Yrs	No. Segmt	No. Flags	Corr w/ Master	Mean msmt	Max msmt	Std dev	Auto corr	Mean sens	Max value	Std dev	Auto corr	AR
53	SP055K	1941	2014	74	3	0	0.446	0.8	1.62	0.355	0.741	0.293	2.71	0.4	0.02	1
54	SP056J	1870	2014	145	6	0	0.483	0.26	0.8	0.131	0.752	0.238	2.86	0.419	-0.033	1
55	SP056K	1870	2014	145	6	1	0.43	0.56	1.35	0.276	0.862	0.212	2.76	0.466	-0.053	1
56	SP059J	1868	2014	147	6	1	0.46	0.6	1.5	0.233	0.735	0.208	2.79	0.407	-0.035	2
57	SP059K	1868	2014	147	6	4	0.321	0.83	2.34	0.386	0.783	0.21	2.86	0.463	0.025	1
58	SP061A	1886	2014	129	5	0	0.471	0.52	1.49	0.227	0.756	0.225	2.73	0.404	-0.043	1
59	SP069J	1924	2014	91	4	0	0.489	0.71	1.7	0.411	0.924	0.203	2.65	0.585	-0.045	1
60	SP069K	1924	2014	91	4	0	0.555	0.59	1.21	0.246	0.809	0.224	2.65	0.458	-0.074	1
61	SP070J	1849	2014	166	7	3	0.337	0.46	1.06	0.232	0.851	0.215	2.71	0.437	-0.043	1
62	SP070K	1849	2014	166	7	3	0.378	0.54	1.47	0.274	0.818	0.23	2.81	0.476	-0.034	7
63	SP071J	1861	2014	154	6	0	0.607	0.5	1.23	0.247	0.767	0.275	2.8	0.443	-0.073	1
64	SP071K	1861	2014	154	6	0	0.542	0.54	1.24	0.253	0.737	0.26	2.73	0.352	-0.05	1
65	SP072A	1878	2014	137	5	1	0.466	0.32	1.32	0.218	0.825	0.306	2.72	0.51	-0.077	1
66	SP072J	1872	2014	143	6	1	0.434	0.38	1.21	0.268	0.854	0.322	2.72	0.395	-0.08	1
67	SP072K	1872	2014	143	6	1	0.523	0.57	1.59	0.292	0.807	0.269	2.78	0.506	-0.078	1
68	SP077J	1919	2014	96	4	0	0.36	0.95	2.88	0.594	0.891	0.201	2.58	0.33	-0.108	3
69	SP077K	1916	2014	99	4	2	0.365	0.64	1.48	0.275	0.707	0.217	2.91	0.432	-0.066	2
70	SP078J	1926	2014	89	3	2	0.339	0.95	1.8	0.296	0.682	0.201	2.99	0.595	-0.004	1

								//---------------- Unfiltered ----------------\\					//--------- Filtered ---------\\			
Seq	Series	Interval		No. Yrs	No. Segmt	No. Flags	Corr w/ Master	Mean msmt	Max msmt	Std dev	Auto corr	Mean sens	Max value	Std dev	Auto corr	AR
71	SP078Y	1953	2014	62	2	0	0.513	0.75	1.23	0.265	0.657	0.206	2.59	0.454	0.066	1
72	SP078Z	1953	2014	62	2	0	0.47	0.83	1.87	0.308	0.719	0.215	2.7	0.425	-0.038	1
73	SP079J	1950	2014	65	2	0	0.464	1.02	2.32	0.339	0.595	0.224	2.92	0.479	0.003	1
74	SP079L	1950	1977	28	1	0	0.442	0.55	1.01	0.166	0.456	0.242	2.73	0.683	0.028	1
75	SP080J	1900	2014	115	4	1	0.362	0.8	2.29	0.435	0.871	0.189	2.51	0.385	-0.005	1
76	SP080M	1908	2014	107	4	2	0.418	0.64	1.12	0.183	0.634	0.191	2.62	0.392	0.041	1
77	SP081J	1925	2014	90	3	1	0.48	0.86	1.52	0.258	0.647	0.192	2.66	0.445	-0.008	1
78	SP083J	1928	2014	87	3	2	0.316	0.43	1.3	0.282	0.895	0.255	2.39	0.301	-0.044	1
79	SP082J	1904	2014	111	4	1	0.386	0.77	1.36	0.271	0.698	0.205	2.41	0.306	-0.072	1
80	SP082K	1904	2014	111	4	1	0.357	0.6	1.28	0.263	0.828	0.21	2.68	0.455	-0.052	1
81	SP083K	1928	2014	87	3	0	0.48	0.54	1.84	0.323	0.862	0.237	2.83	0.474	0.07	1
82	SP084J	1899	2014	116	5	0	0.449	0.6	1.6	0.287	0.805	0.233	2.72	0.455	-0.019	1
83	SP085M	1936	2014	79	3	0	0.506	0.51	1.25	0.282	0.803	0.317	2.46	0.392	-0.021	2
84	SP086K	1911	2014	104	4	0	0.385	0.56	1.06	0.223	0.772	0.23	2.45	0.296	-0.05	1
85	SP087J	1903	2014	112	4	0	0.447	0.41	0.78	0.166	0.811	0.24	2.48	0.371	-0.028	1
86	SP087M	1959	2014	56	2	0	0.522	1	1.56	0.277	0.598	0.204	2.63	0.487	0.049	4
87	SP087Y	1927	2014	88	3	0	0.469	0.73	1.43	0.261	0.765	0.193	2.61	0.442	0.053	1
88	SP087Z	1927	2014	88	3	1	0.42	0.6	1.4	0.239	0.722	0.218	2.58	0.434	-0.08	2

								//------------------ Unfiltered ------------------ -\\					//--------- Filtered ---------\\			
Seq	Series	Interval		No. Yrs	No. Segmt	No. Flags	Corr w/ Master	Mean msmt	Max msmt	Std dev	Auto corr	Mean sens	Max value	Std dev	Auto corr	AR
89	SP089J	1928	2014	87	3	1	0.374	0.51	0.93	0.149	0.634	0.196	2.46	0.334	-0.026	1
90	SP091J	1932	2014	83	3	1	0.374	1.03	1.6	0.278	0.558	0.192	2.6	0.497	0.101	1
91	SP091K	1932	2014	83	3	0	0.384	0.71	1.26	0.172	0.485	0.204	2.69	0.51	-0.035	2
92	SP092J	1919	2014	96	4	0	0.558	0.61	1.12	0.225	0.64	0.236	2.87	0.518	0.027	1
93	SP092M	1943	2014	72	3	1	0.335	0.31	0.6	0.103	0.655	0.218	2.67	0.599	-0.089	1
94	SP094J	1935	2014	80	3	0	0.494	0.74	1.27	0.211	0.426	0.248	2.64	0.45	-0.028	1
95	SP094K	1935	2014	80	3	0	0.505	0.51	0.97	0.181	0.613	0.253	2.7	0.518	0.022	1
96	SP095J	1916	2014	99	4	0	0.574	1.1	2.18	0.322	0.554	0.228	2.65	0.521	0.021	1
97	SP095K	1916	2014	99	4	0	0.54	0.92	1.45	0.236	0.552	0.201	2.45	0.361	-0.001	1
98	SP095Y	1926	2014	89	3	0	0.53	1.18	2.25	0.297	0.538	0.193	2.64	0.454	0.016	1
99	SP095Z	1926	2014	89	3	0	0.473	1.12	1.91	0.275	0.502	0.187	2.7	0.525	0.004	1
100	SP096J	1920	2014	95	4	0	0.515	0.69	2	0.328	0.844	0.182	2.57	0.39	-0.031	1
101	SP096K	1920	2014	95	4	0	0.436	0.87	2.45	0.489	0.891	0.197	2.68	0.424	-0.03	1
102	SP097J	1933	2014	82	3	1	0.318	0.83	1.52	0.273	0.667	0.201	2.98	0.612	0.053	1
103	SP098J	1920	2014	95	4	0	0.532	0.83	1.49	0.263	0.721	0.191	2.46	0.46	0.038	1
104	SP098K	1920	2014	95	4	1	0.447	0.56	1.06	0.17	0.715	0.191	2.59	0.452	-0.055	1
105	SP098Y	1919	2014	96	4	0	0.431	0.66	0.98	0.158	0.536	0.172	2.73	0.547	-0.037	1
106	SP098Z	1919	2014	96	4	0	0.486	0.83	1.3	0.196	0.473	0.19	2.85	0.516	0.043	1

								//---------------- Unfiltered ----------------\\					//--------- Filtered ---------\\			
Seq	Series	Interval		No. Yrs	No. Segmt	No. Flags	Corr w/ Master	Mean msmt	Max msmt	Std dev	Auto corr	Mean sens	Max value	Std dev	Auto corr	AR
107	SP099J	1922	2014	93	4	0	0.499	0.83	1.35	0.215	0.627	0.187	2.7	0.542	0.02	1
108	SP099Y	1927	2014	88	3	0	0.489	0.67	1.61	0.3	0.841	0.204	2.6	0.367	-0.105	1
109	SP100J	1949	2014	66	3	0	0.439	1.42	2.41	0.366	0.661	0.172	2.56	0.445	-0.053	1
110	SP100K	1949	2014	66	3	0	0.316	1.04	1.81	0.297	0.661	0.195	2.45	0.421	-0.012	1
111	SP101M	1881	2014	134	5	1	0.405	0.62	1.39	0.231	0.852	0.15	2.47	0.363	-0.014	1
112	SP103J	1910	2014	105	4	1	0.413	0.57	1.11	0.184	0.624	0.188	2.98	0.433	-0.006	1
113	SP103K	1910	2014	105	4	0	0.472	0.76	1.29	0.276	0.798	0.181	2.52	0.372	-0.086	1
114	SP104K	1880	2014	135	5	0	0.447	0.71	1.4	0.237	0.718	0.182	2.79	0.538	0.022	1
115	SP104Y	1902	2014	113	4	1	0.447	0.65	1.28	0.234	0.794	0.189	2.54	0.476	-0.008	1
116	SP104Z	1902	2014	113	4	0	0.4	0.39	1.05	0.197	0.887	0.18	2.88	0.487	-0.01	1
117	SP106K	1966	2014	49	1	0	0.477	2.18	4.32	1.032	0.531	0.378	2.7	0.509	0.086	1
118	SP109M	1970	2014	45	1	0	0.477	1.96	3.68	0.622	0.674	0.176	2.98	0.652	0.013	1
119	SP110K	1923	2014	92	4	0	0.418	1.6	3.72	0.76	0.857	0.18	2.66	0.458	-0.019	3
120	SP111K	1893	2014	122	5	1	0.393	0.87	1.63	0.272	0.703	0.179	2.64	0.531	0.07	1
121	SP113J	1938	2014	77	3	1	0.427	0.93	3.2	0.531	0.802	0.201	2.61	0.441	-0.048	2
122	SP128J	1868	2014	147	6	1	0.504	0.72	1.97	0.343	0.814	0.222	2.68	0.462	0.044	1
123	SP128K	1868	2014	147	6	4	0.352	0.65	1.95	0.356	0.876	0.189	2.96	0.528	-0.062	1
124	SP129A	1877	2014	138	5	0	0.572	0.73	1.41	0.263	0.771	0.203	2.68	0.426	-0.025	5

								//----------------- Unfiltered -----------------\\					//--------- Filtered ---------\\			
Seq	Series	Interval		No. Yrs	No. Segmt	No. Flags	Corr w/ Master	Mean msmt	Max msmt	Std dev	Auto corr	Mean sens	Max value	Std dev	Auto corr	AR
125	SP132J	1942	2014	73	3	2	0.446	0.93	2.56	0.412	0.818	0.205	2.82	0.469	0.072	1
126	SP132M	1970	2014	45	1	0	0.424	0.54	0.84	0.146	0.656	0.178	2.47	0.524	-0.09	1
127	SP139J	1950	2014	65	2	0	0.556	0.72	1.38	0.239	0.583	0.243	2.69	0.505	0.034	1
128	SP139K	1950	2014	65	2	0	0.436	0.72	1.18	0.264	0.726	0.235	2.61	0.527	0.035	1
129	SP140A	1943	2014	72	3	0	0.426	0.85	1.73	0.363	0.814	0.23	2.74	0.589	-0.059	1
130	SP141A	1953	2014	62	2	0	0.455	1.05	2.92	0.593	0.828	0.273	2.62	0.505	-0.077	1
131	SP142J	1945	2014	70	3	0	0.578	0.84	1.51	0.282	0.745	0.207	2.63	0.564	0.03	1
132	SP143J	1915	2014	100	4	3	0.353	0.6	1.2	0.187	0.604	0.227	2.59	0.427	-0.033	1
133	SP143K	1915	2014	100	4	2	0.422	0.56	1.2	0.309	0.849	0.269	2.65	0.631	-0.038	1
134	SP144J	1952	2014	63	2	0	0.43	0.88	1.52	0.345	0.726	0.237	2.6	0.456	-0.054	1
135	SP145J	1926	2014	89	3	2	0.341	0.59	1.34	0.2	0.505	0.242	2.74	0.517	-0.065	1
136	SP145K	1926	2014	89	3	0	0.456	0.59	1.37	0.226	0.678	0.211	2.85	0.553	0.026	1
137	SP146J	1917	2014	98	4	2	0.359	0.48	1.22	0.212	0.704	0.267	2.58	0.401	-0.05	4
138	SP147J	1908	2014	107	4	2	0.428	0.49	1.4	0.243	0.675	0.263	3.04	0.425	-0.121	1
139	SP147K	1908	2014	107	4	0	0.406	0.66	1.84	0.406	0.875	0.221	2.78	0.457	0.02	1
140	SP148J	1866	2014	149	6	1	0.474	0.34	0.83	0.175	0.852	0.206	2.6	0.387	-0.031	1
141	SP148K	1866	2014	149	6	1	0.454	0.44	1	0.217	0.883	0.174	2.66	0.365	-0.009	1
142	SP149J	1849	2014	166	7	1	0.471	0.52	1.13	0.228	0.876	0.19	2.47	0.335	0.005	1

								//---------------- Unfiltered ----------------\\					//--------- Filtered ---------\\			
Seq	Series	Interval		No. Yrs	No. Segmt	No. Flags	Corr w/ Master	Mean msmt	Max msmt	Std dev	Auto corr	Mean sens	Max value	Std dev	Auto corr	AR
143	SP149L	1849	1962	114	5	0	0.474	0.41	1.06	0.149	0.794	0.171	2.72	0.427	0.095	1
144	SP150J	1890	2014	125	5	2	0.478	0.43	0.84	0.189	0.826	0.213	2.64	0.431	-0.026	1
145	SP150K	1890	2014	125	5	1	0.484	0.32	0.6	0.104	0.717	0.195	2.73	0.477	-0.06	1
146	SP153K	1925	2014	90	3	0	0.389	0.87	2.13	0.407	0.804	0.21	2.55	0.383	-0.018	1
147	SP161J	1863	2014	152	6	3	0.378	0.4	1.13	0.217	0.822	0.239	2.6	0.361	-0.094	1
148	SP161K	1863	2014	152	6	2	0.355	0.38	1.13	0.22	0.758	0.261	2.76	0.439	-0.051	1
149	SP162J	1932	2014	83	3	0	0.467	0.71	1.91	0.382	0.776	0.291	2.51	0.327	-0.033	1
150	SP163J	1918	2014	97	4	0	0.496	0.58	1.56	0.281	0.699	0.286	2.63	0.434	-0.003	1
151	SP163K	1918	2014	97	4	0	0.45	0.61	1.76	0.298	0.631	0.307	2.7	0.359	-0.072	2
152	SP164J	1912	2014	103	4	0	0.469	0.46	1.43	0.269	0.618	0.368	2.6	0.362	-0.111	1
153	SP165J	1945	2014	70	3	1	0.492	0.53	1.09	0.22	0.642	0.239	2.43	0.33	-0.096	1
154	SP165K	1945	2014	70	3	2	0.37	0.46	1.14	0.256	0.787	0.345	2.53	0.4	-0.01	1
155	SP168J	1916	2014	99	4	0	0.462	0.54	1.37	0.261	0.781	0.235	2.76	0.419	0.022	1
156	SP168K	1916	2014	99	4	0	0.511	0.58	1.29	0.243	0.752	0.238	2.52	0.383	-0.09	1
157	SP105J	1882	2014	133	5	3	0.31	0.6	1.16	0.157	0.567	0.191	2.76	0.48	-0.029	2
158	SP105K	1882	2014	133	5	3	0.327	0.42	1.17	0.147	0.735	0.185	2.7	0.468	-0.003	1
159	SP108J	1949	2014	66	3	3	0.304	0.8	1.88	0.418	0.82	0.23	2.72	0.519	-0.045	2

Table S-3. ARSTAN Output. Detrending options (LR = linear regression; NEC = negative exponential curve) and coefficients; Auto-regression coefficients for each core series.

Negative exponential curve: $f(i) = a*exp(-b*t(i)) + d$ (any d)

Linear regression (any slope): $f(i) = +/-c*t(i) + d$

		//------------------ Detrend Coeff -------------------\\					//---------AR Coeff ---------\\			
Seq	**Series**	**Option**	**a**	**b**	**c**	**d**	**rsq**	**t-1**	**t-2**	**t-3**
1	SP001J	LR	0.00E+00	0.00E+00	1.45E-03	4.62E-01	0.312	0.56	-0.084	0.107
2	SP001K	LR	0.00E+00	0.00E+00	2.61E-03	5.21E-01	0.193	0.453	-0.046	0.019
3	SP002J	LR	0.00E+00	0.00E+00	1.38E-03	4.14E-01	0.548	0.686	0.032	0.049
4	SP002K	NEC	4.19E-01	1.62E-04	0.00E+00	4.13E-02	0.505	0.73	-0.079	0.059
5	SP003A	NEC	1.80E+01	3.41E-04	0.00E+00	6.71E+00	0.611	0.634	0.091	0.088
6	SP004J	NEC	5.92E-01	8.67E-04	0.00E+00	7.86E-02	0.426	0.532	0.103	0.083
7	SP004K	NEC	5.19E-01	8.22E-02	0.00E+00	5.52E-01	0.337	0.485	0.038	0.141
8	SP007J	NEC	4.20E-01	7.73E-02	0.00E+00	3.62E-01	0.522	0.806	-0.145	0.034
9	SP007K	NEC	7.87E-01	1.73E-03	0.00E+00	2.26E-02	0.378	0.648	-0.046	-0.022
10	SP007Y	NEC	1.64E+01	2.01E-04	0.00E+00	5.53E+00	0.481	0.602	0.162	-0.05
11	SP007Z	NEC	2.39E+00	4.34E-04	0.00E+00	1.85E+00	0.382	0.626	-0.032	-0.024
12	SP008J	NEC	2.77E-01	1.04E-01	0.00E+00	3.17E-01	0.455	0.449	0.253	0.043
13	SP009K	NEC	3.93E-01	5.61E-03	0.00E+00	6.41E-02	0.56	0.61	-0.04	0.246
14	SP011J	LR	0.00E+00	0.00E+00	2.51E-02	9.28E-01	0.259	0.548	-0.13	0.035
15	SP011K	LR	0.00E+00	0.00E+00	1.12E-02	8.68E-01	0.264	0.054	-0.055	-0.494
16	SP016J	NEC	4.55E-01	1.46E-02	0.00E+00	2.74E-01	0.606	0.759	-0.072	0.119
17	SP016K	NEC	7.55E-01	1.29E-01	0.00E+00	2.96E-01	0.342	0.527	0.06	0.007
18	SP017K	NEC	7.12E-01	2.29E-02	0.00E+00	4.35E-01	0.371	0.526	0.146	-0.035
19	SP019J	LR	0.00E+00	0.00E+00	5.16E-04	7.23E-01	0.656	0.818	-0.023	-0.004
20	SP019K	LR	0.00E+00	0.00E+00	1.11E-03	6.81E-01	0.538	0.609	0.186	-0.035
21	SP020J	NEC	7.80E-01	1.84E-03	0.00E+00	1.69E-02	0.561	0.756	-0.061	0.048
22	SP020K	NEC	6.74E-01	8.33E-02	0.00E+00	5.17E-01	0.483	0.779	-0.262	0.163
23	SP021J	LR	0.00E+00	0.00E+00	1.16E-03	2.97E-01	0.616	0.77	0.071	-0.093
24	SP021K	LR	0.00E+00	0.00E+00	7.53E-04	3.33E-01	0.553	0.658	0.148	-0.048
25	SP023J	NEC	9.38E-01	1.78E-03	0.00E+00	3.58E-02	0.343	0.646	-0.233	0.18
26	SP023K	NEC	6.13E-01	8.81E-04	0.00E+00	4.00E-02	0.228	0.515	-0.188	-0.047
27	SP024A	LR	0.00E+00	0.00E+00	6.58E-03	7.56E-01	0.415	0.604	-0.014	0.099
28	SP024B	LR	0.00E+00	0.00E+00	7.56E-04	8.14E-01	0.378	0.628	-0.073	0.076

		//------------------ Detrend Coeff ------------------\\					//---------AR Coeff ---------\\			
Seq	**Series**	**Option**	**a**	**b**	**c**	**d**	**rsq**	**t-1**	**t-2**	**t-3**
29	SP025J	NEC	9.34E-01	4.43E-03	0.00E+00	3.77E-01	0.52	0.703	0.038	-0.019
30	SP025K	NEC	1.09E+00	1.56E-02	0.00E+00	9.89E-02	0.636	0.91	-0.212	0.086
31	SP026J	LR	0.00E+00	0.00E+00	1.44E-03	2.53E-01	0.422	0.602	0.026	0.058
32	SP026K	LR	0.00E+00	0.00E+00	6.25E-03	2.36E-01	0.389	0.642	-0.099	0.101
33	SP029K	NEC	8.37E-01	1.79E-03	0.00E+00	1.27E-02	0.548	0.589	0.203	-0.014
34	SP030K	NEC	4.70E-01	1.19E-02	0.00E+00	1.81E-01	0.731	0.979	-0.159	0.01
35	SP032J	NEC	5.18E+00	1.83E-04	0.00E+00	4.77E+00	0.528	0.74	0.009	-0.041
36	SP032K	LR	0.00E+00	0.00E+00	7.30E-04	6.45E-01	0.634	0.75	-0.031	0.092
37	SP035J	LR	0.00E+00	0.00E+00	3.50E-04	8.20E-01	0.461	0.447	0.179	0.145
38	SP035K	NEC	1.01E+00	9.97E-03	0.00E+00	1.98E-03	0.392	0.652	-0.04	-0.011
39	SP038J	NEC	5.39E-01	3.89E-03	0.00E+00	2.73E-02	0.463	0.563	0.121	0.048
40	SP038K	LR	0.00E+00	0.00E+00	2.50E-03	2.85E-01	0.39	0.562	0.035	0.071
41	SP039J	NEC	8.69E-01	7.57E-02	0.00E+00	5.80E-01	0.497	0.51	0.207	0.047
42	SP039K	NEC	1.00E+00	6.35E-02	0.00E+00	4.06E-01	0.399	0.432	0.125	0.156
43	SP040J	LR	0.00E+00	0.00E+00	1.05E-03	5.37E-01	0.517	0.743	-0.087	0.072
44	SP040K	NEC	6.30E-01	8.67E-04	0.00E+00	3.83E-02	0.369	0.484	0.035	0.152
45	SP041J	LR	0.00E+00	0.00E+00	2.15E-04	3.17E-01	0.649	0.851	-0.135	0.087
46	SP047J	LR	0.00E+00	0.00E+00	6.87E-03	2.81E-01	0.504	0.752	-0.137	0.104
47	SP053J	NEC	7.28E-01	6.19E-03	0.00E+00	1.56E-02	0.573	0.882	-0.2	0.032
48	SP053K	LR	0.00E+00	0.00E+00	8.20E-04	4.79E-01	0.711	0.863	-0.096	0.082
49	SP054J	LR	0.00E+00	0.00E+00	1.05E-03	3.59E-01	0.551	0.654	0.109	0.005
50	SP054K	LR	0.00E+00	0.00E+00	3.45E-03	2.29E-01	0.655	0.763	0.15	-0.118
51	SP054Y	LR	0.00E+00	0.00E+00	2.63E-03	4.49E-01	0.67	0.793	-0.149	0.203
52	SP054Z	LR	0.00E+00	0.00E+00	2.57E-04	4.04E-01	0.59	0.646	0.192	-0.05
53	SP055K	LR	0.00E+00	0.00E+00	1.03E-02	4.19E-01	0.434	0.757	-0.286	0.183
54	SP056J	NEC	6.51E-01	2.67E-01	0.00E+00	2.49E-01	0.532	0.743	-0.043	0.033
55	SP056K	LR	0.00E+00	0.00E+00	1.34E-03	4.64E-01	0.728	0.712	0.146	0.016
56	SP059J	LR	0.00E+00	0.00E+00	1.33E-03	5.01E-01	0.542	0.795	-0.21	0.168
57	SP059K	LR	0.00E+00	0.00E+00	4.69E-03	4.81E-01	0.498	0.672	0.101	-0.086
58	SP061A	NEC	2.10E+01	1.19E-04	0.00E+00	3.38E-01	0.489	0.75	-0.105	0.043
59	SP069J	NEC	1.53E+00	1.94E-02	0.00E+00	8.00E-05	0.496	0.484	0.196	0.088
60	SP069K	NEC	4.75E-01	1.01E-01	0.00E+00	5.45E-01	0.622	0.816	0.036	-0.109
61	SP070J	LR	0.00E+00	0.00E+00	2.82E-03	2.28E-01	0.595	0.735	0.012	0.043
62	SP070K	LR	0.00E+00	0.00E+00	1.22E-03	4.36E-01	0.669	0.662	0.257	-0.086
63	SP071J	LR	0.00E+00	0.00E+00	1.35E-03	3.97E-01	0.598	0.683	0.123	-0.029
64	SP071K	LR	0.00E+00	0.00E+00	2.62E-03	3.36E-01	0.495	0.663	0.106	-0.09
65	SP072A	NEC	1.67E+00	3.57E-01	0.00E+00	2.95E-01	0.585	0.792	0.015	-0.084
66	SP072J	NEC	1.09E+00	1.49E-01	0.00E+00	3.30E-01	0.705	0.801	0.219	-0.233

		//------------------ Detrend Coeff ------------------\\					//---------AR Coeff ---------\\			
Seq	**Series**	**Option**	**a**	**b**	**c**	**d**	**rsq**	**t-1**	**t-2**	**t-3**
67	SP072K	NEC	5.46E-01	7.04E-04	0.00E+00	5.39E-02	0.658	0.687	0.055	0.104
68	SP077J	LR	0.00E+00	0.00E+00	1.20E-02	3.67E-01	0.755	1.109	-0.369	0.089
69	SP077K	NEC	7.08E-01	3.74E-03	0.00E+00	5.19E-02	0.438	0.689	-0.12	0.112
70	SP078J	LR	0.00E+00	0.00E+00	2.81E-03	8.26E-01	0.473	0.67	0.097	-0.152
71	SP078Y	LR	0.00E+00	0.00E+00	5.62E-03	5.73E-01	0.427	0.543	0.04	0.141
72	SP078Z	LR	0.00E+00	0.00E+00	8.82E-03	5.55E-01	0.45	0.65	0.067	-0.056
73	SP079J	LR	0.00E+00	0.00E+00	4.68E-03	8.64E-01	0.356	0.629	-0.053	-0.116
74	SP079L	NEC	5.16E-01	2.56E-03	0.00E+00	5.44E-02	0.222	0.44	0.092	-0.125
75	SP080J	LR	0.00E+00	0.00E+00	9.82E-03	2.29E-01	0.652	0.79	0.05	-0.043
76	SP080M	NEC	6.03E-01	1.68E-04	0.00E+00	4.54E-02	0.407	0.624	0.076	-0.093
77	SP081J	LR	0.00E+00	0.00E+00	2.50E-04	8.46E-01	0.429	0.658	-0.082	0.106
78	SP083J	NEC	6.20E-01	3.81E-02	0.00E+00	2.53E-01	0.684	0.673	0.341	-0.192
79	SP082J	LR	0.00E+00	0.00E+00	3.62E-03	5.68E-01	0.428	0.546	0.13	0.024
80	SP082K	NEC	7.46E-01	5.73E-03	0.00E+00	4.78E-02	0.629	0.767	0.095	-0.089
81	SP083K	LR	0.00E+00	0.00E+00	4.76E-03	3.31E-01	0.705	0.798	0.088	-0.047
82	SP084J	LR	0.00E+00	0.00E+00	5.13E-03	3.02E-01	0.519	0.584	0.023	0.176
83	SP085M	NEC	6.90E-01	1.02E-02	0.00E+00	4.23E-02	0.607	0.909	-0.176	-0.01
84	SP086K	LR	0.00E+00	0.00E+00	1.01E-03	5.12E-01	0.606	0.687	0.159	-0.057
85	SP087J	NEC	3.84E-01	5.53E-02	0.00E+00	3.46E-01	0.611	0.572	0.246	0.007
86	SP087M	LR	0.00E+00	0.00E+00	2.10E-03	9.43E-01	0.406	0.667	-0.047	-0.198
87	SP087Y	NEC	8.12E-01	5.86E-02	0.00E+00	5.82E-01	0.278	0.478	0.067	0.027
88	SP087Z	NEC	5.15E-01	9.99E-02	0.00E+00	5.47E-01	0.528	0.886	-0.263	0.001
89	SP089J	LR	0.00E+00	0.00E+00	9.60E-05	5.04E-01	0.407	0.599	0.09	-0.049
90	SP091J	NEC	1.02E+00	1.20E-05	0.00E+00	1.49E-02	0.346	0.466	0.032	0.187
91	SP091K	NEC	6.52E-01	6.49E-04	0.00E+00	7.42E-02	0.243	0.507	-0.086	0.09
92	SP092J	NEC	6.24E-01	2.52E-03	0.00E+00	6.01E-02	0.414	0.58	-0.036	0.154
93	SP092M	NEC	3.19E-01	1.62E-01	0.00E+00	2.89E-01	0.359	0.55	0.171	-0.252
94	SP094J	NEC	3.73E-01	3.65E-02	0.00E+00	6.24E-01	0.141	0.199	0.223	0.025
95	SP094K	NEC	4.35E-01	1.08E-01	0.00E+00	4.62E-01	0.263	0.408	0.114	0.067
96	SP095J	LR	0.00E+00	0.00E+00	3.06E-04	1.09E+00	0.318	0.529	0.005	0.073
97	SP095K	LR	0.00E+00	0.00E+00	5.07E-04	8.91E-01	0.327	0.57	-0.072	0.091
98	SP095Y	NEC	1.23E+00	1.97E-03	0.00E+00	5.74E-02	0.326	0.341	0.186	0.165
99	SP095Z	LR	0.00E+00	0.00E+00	8.22E-04	1.09E+00	0.264	0.436	0.097	0.05
100	SP096J	NEC	1.00E+00	6.14E-02	0.00E+00	5.22E-01	0.528	0.725	0.023	-0.039
101	SP096K	NEC	1.47E+00	3.28E-02	0.00E+00	4.26E-01	0.632	0.66	0.217	-0.073
102	SP097J	NEC	1.82E+00	1.58E-03	0.00E+00	8.71E-01	0.465	0.458	0.098	0.222
103	SP098J	NEC	8.31E+00	4.10E-04	0.00E+00	7.32E+00	0.453	0.659	-0.005	0.031
104	SP098K	NEC	4.89E-01	4.13E-02	0.00E+00	4.41E-01	0.225	0.449	0.089	-0.117

		//------------------ Detrend Coeff -------------------\\					//---------AR Coeff ---------\\			
Seq	**Series**	**Option**	**a**	**b**	**c**	**d**	**rsq**	**t-1**	**t-2**	**t-3**
105	SP098Y	NEC	6.79E-01	2.31E-03	0.00E+00	4.78E-02	0.283	0.556	-0.034	-0.046
106	SP098Z	LR	0.00E+00	0.00E+00	2.16E-03	7.23E-01	0.169	0.378	0.004	0.098
107	SP099J	NEC	4.01E+00	1.30E-03	0.00E+00	2.94E+00	0.196	0.382	-0.012	0.12
108	SP099Y	NEC	1.06E+00	1.59E-02	0.00E+00	9.86E-02	0.463	0.542	0.2	-0.029
109	SP100J	NEC	1.50E+00	1.93E-03	0.00E+00	1.21E-02	0.473	0.624	-0.051	0.163
110	SP100K	NEC	9.31E-01	7.60E-02	0.00E+00	8.61E-01	0.069	0.227	0.022	0.012
111	SP101M	LR	0.00E+00	0.00E+00	5.65E-04	5.79E-01	0.733	0.88	-0.091	0.07
112	SP103J	NEC	1.07E+00	1.09E-03	0.00E+00	4.45E-01	0.41	0.471	0.318	-0.127
113	SP103K	LR	0.00E+00	0.00E+00	4.02E-03	5.50E-01	0.65	0.608	0.196	0.037
114	SP104K	NEC	1.66E+00	2.84E-03	0.00E+00	6.70E-01	0.436	0.436	0.06	0.266
115	SP104Y	NEC	8.20E-01	6.15E-03	0.00E+00	6.26E-02	0.571	0.642	0.011	0.157
116	SP104Z	NEC	6.98E-01	2.36E-02	0.00E+00	1.44E-01	0.291	0.356	0.073	0.232
117	SP106K	LR	0.00E+00	0.00E+00	2.36E-02	1.59E+00	0.268	0.493	0.054	-0.023
118	SP109M	LR	0.00E+00	0.00E+00	3.03E-02	1.27E+00	0.273	0.429	0.223	-0.284
119	SP110K	LR	0.00E+00	0.00E+00	2.26E-02	5.46E-01	0.609	0.523	0.372	-0.077
120	SP111K	LR	0.00E+00	0.00E+00	1.76E-03	7.60E-01	0.464	0.638	0.049	0.011
121	SP113J	NEC	9.70E-01	1.38E-03	0.00E+00	1.13E-02	0.692	1.097	-0.369	0.005
122	SP128J	LR	0.00E+00	0.00E+00	2.05E-04	7.09E-01	0.666	0.805	-0.068	0.093
123	SP128K	NEC	1.30E+00	5.68E-02	0.00E+00	4.98E-01	0.622	0.633	0.092	0.11
124	SP129A	LR	0.00E+00	0.00E+00	2.70E-03	5.40E-01	0.533	0.701	-0.069	0.132
125	SP132J	NEC	1.84E+00	1.55E-01	0.00E+00	7.84E-01	0.362	0.656	-0.121	0.036
126	SP132M	LR	0.00E+00	0.00E+00	3.06E-03	4.74E-01	0.496	0.405	0.123	0.255
127	SP139J	NEC	7.41E-01	2.59E-03	0.00E+00	3.71E-02	0.367	0.584	0.083	-0.176
128	SP139K	NEC	3.15E+01	3.29E-04	0.00E+00	3.89E-01	0.149	0.276	0.13	0.033
129	SP140A	NEC	1.12E+00	2.77E-02	0.00E+00	3.74E-01	0.408	0.483	0.021	0.233
130	SP141A	NEC	1.85E+00	1.75E-02	0.00E+00	6.94E-02	0.452	0.657	0.095	-0.133
131	SP142J	NEC	9.83E+00	1.04E-03	0.00E+00	8.64E+00	0.245	0.451	0.131	-0.125
132	SP143J	LR	0.00E+00	0.00E+00	1.15E-03	5.45E-01	0.408	0.442	0.191	0.095
133	SP143K	NEC	2.32E+01	1.20E-04	0.00E+00	2.51E+00	0.712	0.519	0.333	0.034
134	SP144J	NEC	9.51E-01	3.13E-03	0.00E+00	1.69E-02	0.536	0.643	0.226	-0.148
135	SP145J	NEC	5.38E-01	1.92E-03	0.00E+00	9.99E-02	0.26	0.469	0.043	0.028
136	SP145K	NEC	5.75E-01	3.91E-03	0.00E+00	1.01E-01	0.449	0.67	0.072	-0.125
137	SP146J	LR	0.00E+00	0.00E+00	4.82E-04	4.52E-01	0.518	0.819	-0.113	-0.1
138	SP147J	LR	0.00E+00	0.00E+00	2.58E-03	3.49E-01	0.472	0.604	0.19	-0.107
139	SP147K	LR	0.00E+00	0.00E+00	8.34E-03	2.09E-01	0.753	0.811	-0.089	0.165
140	SP148J	LR	0.00E+00	0.00E+00	1.20E-03	2.52E-01	0.732	0.701	0.127	0.054
141	SP148K	LR	0.00E+00	0.00E+00	3.45E-03	1.79E-01	0.673	0.769	-0.066	0.145
142	SP149J	LR	0.00E+00	0.00E+00	8.86E-04	4.42E-01	0.775	0.703	0.119	0.081

		//------------------ Detrend Coeff -------------------\\					//---------AR Coeff ---------\\			
Seq	Series	Option	a	b	c	d	rsq	t-1	t-2	t-3
143	SP149L	LR	0.00E+00	0.00E+00	1.53E-03	3.19E-01	0.59	0.687	0.071	0.038
144	SP150J	LR	0.00E+00	0.00E+00	2.85E-03	2.50E-01	0.617	0.559	0.124	0.164
145	SP150K	LR	0.00E+00	0.00E+00	1.58E-03	2.18E-01	0.397	0.637	-0.138	0.172
146	SP153K	LR	0.00E+00	0.00E+00	1.15E-02	3.43E-01	0.39	0.618	0.029	-0.061
147	SP161J	LR	0.00E+00	0.00E+00	1.92E-03	2.55E-01	0.621	0.808	0.004	-0.043
148	SP161K	LR	0.00E+00	0.00E+00	1.98E-03	2.27E-01	0.526	0.796	-0.089	-0.021
149	SP162J	LR	0.00E+00	0.00E+00	4.46E-03	5.19E-01	0.614	0.772	-0.039	0.052
150	SP163J	NEC	7.09E-01	6.96E-03	0.00E+00	6.87E-02	0.428	0.684	-0.124	0.109
151	SP163K	NEC	9.12E-01	9.97E-03	0.00E+00	3.26E-02	0.346	0.607	-0.032	-0.058
152	SP164J	NEC	2.27E+00	3.50E-04	0.00E+00	1.77E+00	0.408	0.619	0.12	-0.211
153	SP165J	NEC	6.21E-01	2.07E-01	0.00E+00	4.92E-01	0.401	0.52	0.165	-0.071
154	SP165K	NEC	4.07E+00	8.69E-04	0.00E+00	3.49E+00	0.598	0.881	-0.095	-0.138
155	SP168J	NEC	8.12E+00	2.05E-04	0.00E+00	7.50E+00	0.593	0.726	0.089	-0.051
156	SP168K	NEC	5.50E-01	2.94E-03	0.00E+00	1.02E-01	0.532	0.642	0.106	0.009
157	SP105J	NEC	6.33E-01	2.13E-03	0.00E+00	4.73E-02	0.317	0.547	-0.108	0.172
158	SP105K	NEC	3.16E+00	6.96E-04	0.00E+00	2.60E+00	0.385	0.528	-0.01	0.166
159	SP108J	LR	0.00E+00	0.00E+00	1.01E-02	4.59E-01	0.651	0.8	0.048	-0.051

7.2 Supplemental Figures

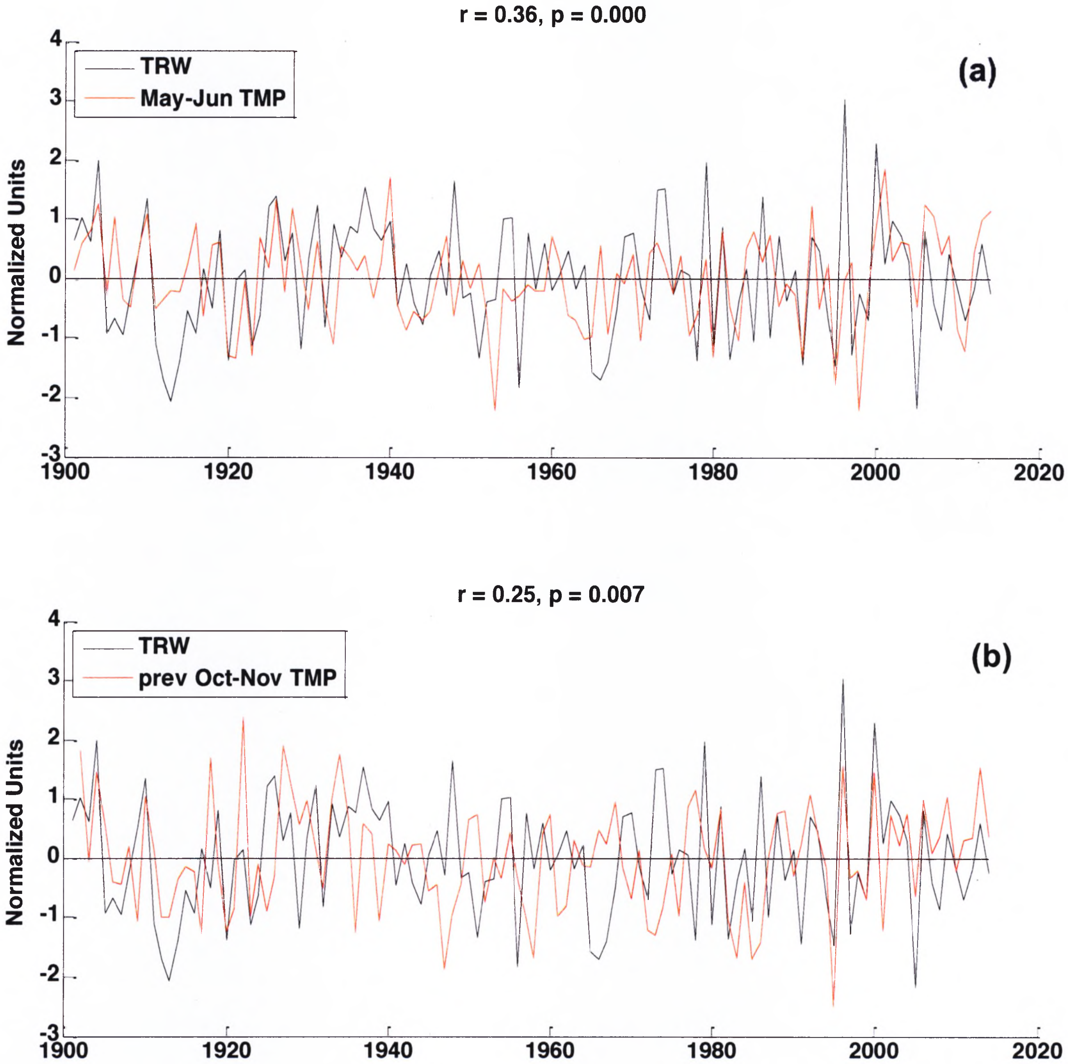

Supplemental Fig S-1. Normalized time series of TRW and CRU average temperature. (a) Early summer temperature represented by an average of May and Jun monthly temperatures. **(b)** Late-fall temperature represented by an average of pOct and Nov monthly temperatures.

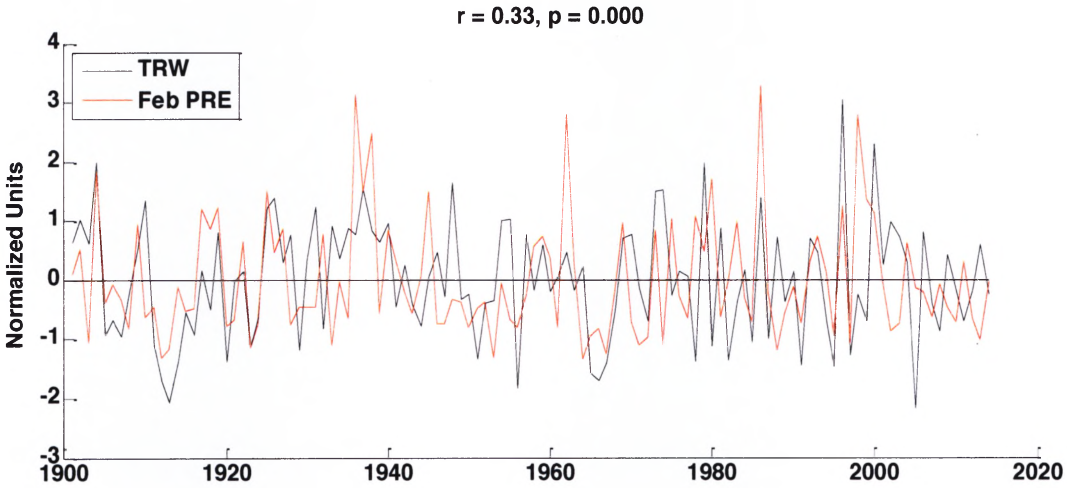

Supplemental Fig S-2. Normalized time series of residual ring width (black) and local February precipitation (red).

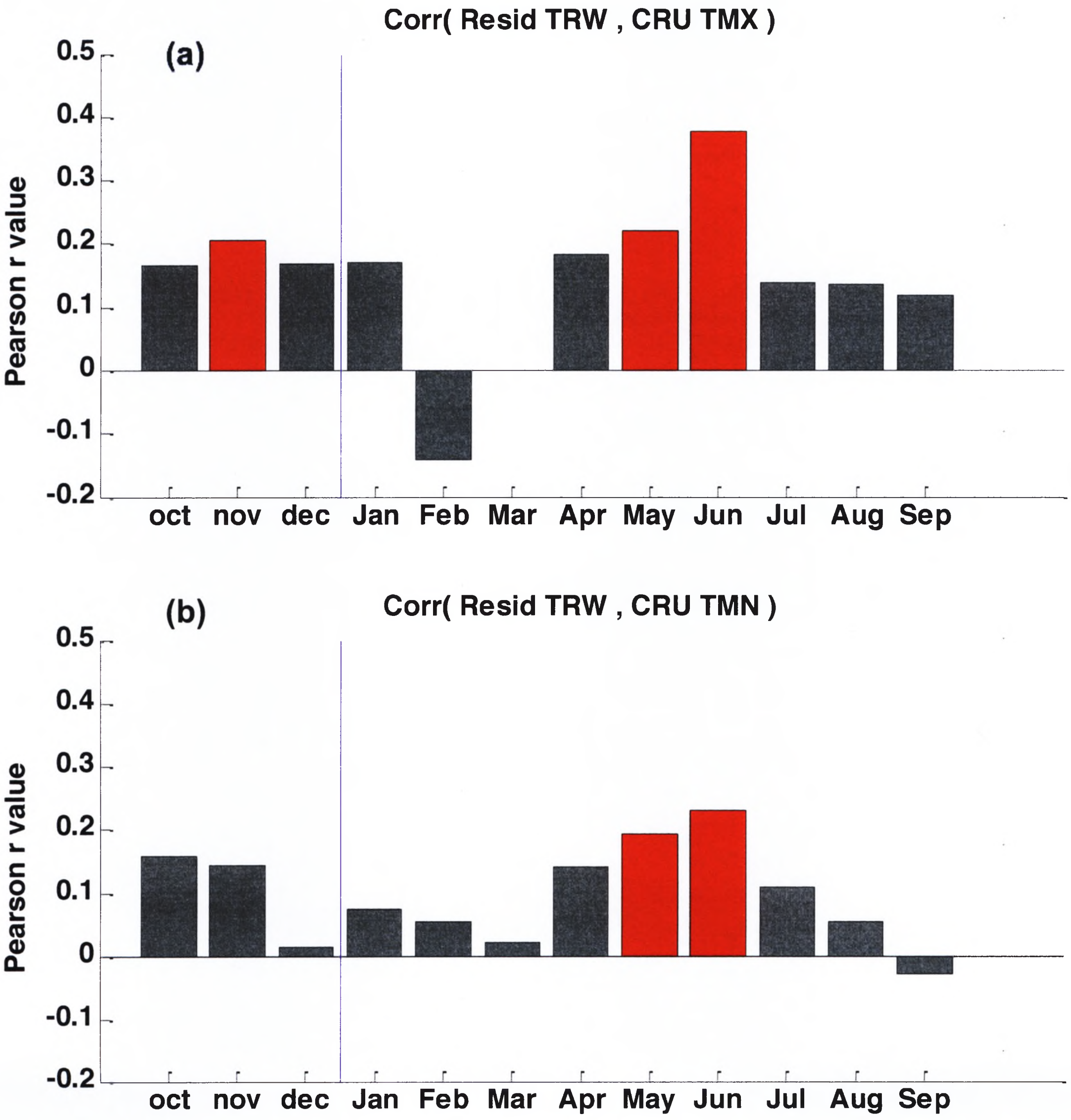

Supplemental Fig S-3. Correlation between TRW and (a) monthly maximum temperature (TMX), and (b) monthly minimum temperature (TMN) from pOct to Sep. Significant correlations ($p < 0.05$) are highlighted in red.

This page is intentionally left blank.

CHAPTER 2

Influence of Inter-Tree Competition on Growth at a High Sierra Treeline Environment

ABSTRACT

Tree growth at treeline tends to covary with temperature variability often forms the basis for past temperature reconstruction. However the strong covariance between growing season temperature and solar radiation permit ambiguity in attribution. Large-scale light availability has been demonstrated to influence tree-ring series used to infer temperature. Here we experimentally test the effects of tree-scale shading variabilities on treeline growth by mapping and coring 178 trees across a study site near Sonora Pass, CA (38.32N, 119.64W; elev. 3130m). The tree-ring width chronology shows significant, positive correlations with May-Jun temperature ($r = 0.36$, $p < 0.001$), suggesting a temperature-limited environment. Inter-tree shading is represented by a competition index calculated using size and position measurements of each tree and its neighbors. We show that differences in growth rate between trees are predicted by competition ($r = -0.46$, $p < 0.001$). Moreover, trees with taller neighbors and neighbors to the south experience greater competition stress on growth than those with shorter or northerly neighbors, indicating that competition for incident radiation exists and light availability likely poses a control on growth at treeline environments.

1. INTRODUCTION

1.1. Controls on Growth at Treeline

There exist a wide range of hypotheses on the cause of the position of a treeline. Aside from topographic constraints or anthropogenic influences, a natural climatic treeline is typically defined as the uppermost elevation where upright standing trees show strong deterioration in statue and density but remain at least 3 m in height and grow in groups (Korner and Paulsen, 2004; Holtmeier and Broll, 2005; Holtmeier, 2009). Low temperature during the growing season (Hoch and Korner, 2009), length of the growing season (Hadley and Smith, 1990), tree mortality due to winter desiccation or freezing and mechanical damages (Tranquillini, 1979; Pereg & Payette, 1998), and seedling viability from temperature and moisture stresses (Malanson, 1997) are among the climatic causes determining treeline positions. While some studies argue that regional variabilities or types of treeline contribute to different climate response (Harsch and Bader, 2011), others suggests a common signal (e.g. soil temperature) predicts treeline location across the globe consistently (Korner and Paulsen, 2004; Hoch and Korner, 2009). Whether these factors relate to summer temperature limitation or winter stress, there is general consensus that growth at such delicate environments are sensitive to climate variability. Growth response studies – primarily using tree-rings – at treeline has allowed for countless number of climate reconstructions across the globe and provided important understanding of our past climate (e.g. Briffa et al, 1992).

Although trees from a given region are subject to the same large-scale climatic environment, the absolute tree-ring with (TRW) measurements (a common surrogate for growth) between trees sampled across a site often contain large variations. Standard dendroclimatology protocol conventionally removes the trend in each tree-ring time series and averages all trees to extract a common climate signal and treats the between-tree variations as noise. If different forms of treeline respond to different climate controls (Harsch and Bader, 2011), it begs the question: does individual-level variation affect the sensitivity of the tree to climate variabilities? In other words, can we identify tree-scale factor(s) to explain the between-tree noise which also influences radial growth? One such factor is that treeline trees take various forms, sizes, and groupings, and they exert or experience different levels of competition stress on or from their neighbors. Quantifying the degree to which competition modulates tree growth are critical to improving our understanding of how treeline trees respond to climate variability. Additionally, determining what controls competition allows us to selectively sample trees to increase the signal-to-noise ratios of the desired reconstruction.

1.2. Light Hypothesis

Tree growth is typically a function of multiple environmental factors. Existing literature in dendroclimatology practice is generally based on Liebig’s Law of the Minimum (Stokes and Smiley, 1968; Speer, 2010), which says trees that grow in extreme environments where the factor that is most limiting on growth locally will control tree growth. In particular, the Vaganov-Shashkin model of growth and tree-ring formation (Eq. 1; Vaganov et al., 2006) scales tree growth ($G(t)$) with the amount of light available and is limited by either temperature or water availability.

Equation 1 $$G(t) = g_E(t) \times min\{g_T(t), g_W(t)\}$$

Partial growth rates for solar irradiation ($g_E(t)$), temperature ($g_T(t)$), and soil water content ($g_W(t)$) are determined independently. According to this model, it can be conjectured that tree ring records from cold climates respond to temperature variabilities, but light availability may act as a modulating factor.

Recent work has also shown that large-scale light reduction as a result of volcanism and global dimming contributes to growth declines recorded by high-latitude tree-ring records commonly used for temperature reconstruction (Stine & Huybers 2016, Tingley et al 2014). When comparing tree ring-derived temperature variabilities to instrumental records for Novarupta and Krakatau, two large volcanic eruptions in recent history, the ring records tended to overestimate cooling following an eruption, suggesting that trees might be responding to more than a decrease in temperature (Tingley et al., 2014). It is well understood that large eruption events deposit volcanic ash into the stratosphere. Because the stratosphere is convectively stable, the ash can spread out and stay in the upper atmosphere for months to years. The ash particles scatter incoming sunlight, which not only cools but also reduces the amount of direct light reaching the

Earth's surface. Furthermore, gathering from latewood density response to 15 large volcanic eruptions, trees growing in cloudy regions of the Arctic yielded a greater decrease in latewood density following an eruption than those in clear regions (Stine and Huybers, 2014), suggesting that trees from low-light background environments are more sensitive to reductions in light and temperature. While light reduction following volcanism generally lasts a few years, similar patterns were also observed over a longer period (approximately 1955-1975) of reduced shortwave radiation known as global dimming (Stine and Huybers, 2014). Tree-ring density records from cloudy regions again showed the most negative and significant trend, and its magnitude was significantly correlated with light limitation (Stine and Huybers, 2014).

These studies compiled existing tree-ring data (Scheweingruber and Briffa, 1996) and demonstrated the influence of light on treeline growth by comparing the differences in the large-scale spatial response of tree-ring series between sites. Here we build upon this idea to experimentally test for the influence of light availability on growth at the individual tree level. Using tree cores collected at a treeline site near Sonora Pass, CA, we developed a TRW chronology following standard dendrochronology protocols (Stokes and Smiley, 1968). The chronology significantly and positively correlates with May-June instrumental temperature records ($r = 0.36$, $p < 0.01$; Ma et al., in preparation), consistent with findings from other Sierra treeline environments. We further calculate a competition index for each tree to quantify inter-tree variabilities under the hypothesis that shading from neighbor trees influences growth. Our findings provide a direct test on the possibility of multiple factors affecting growth in cold climates as well as the potential of light limitation on trees selected for temperature reconstruction.

2. METHODS

2.1. Site Selection

We selected a study site near Sonora Pass, California (Fig. 1a; 38.32N, 119.64W, 3130m) because it offers a treeline environment and contains relatively flat area ideal for controlling non-temperature variables and testing hypotheses. This 80m x 70m site sits on part of a cirque bounded by sharp cliff drops on the west, north, and east sides, and by a peak of 3353 meters rising precipitously to the south (Fig 1a). Multiple streams run around and through the area. The only tree species identified is whitebark pines (*Pinus albicaulis*), a common treeline species in the Sierra Nevada. It is visually apparent that trees in this region are increasingly stressed with elevation. Our study area hosts some of the highest, upright standing forest patches in the surrounding mountain slopes; the trees grow in tree-form but have a gnarred appearance (Fig. 1b). Nearby trees located approximately 50 meters higher in elevation grow exclusively as isolated individuals or in krummholtz form. Lower-elevation trees growing approximately 30 meters below the site are taller, thicker, and do not show the level of visual stress seen at the study site. These attributes of the site suggest that temperature variability is likely to play in important role in governing year-to-year variability in growth at our study location. Additionally, trees in our study area form varying-size patches across the site, providing an opportunity to test spatial clustering effects related to water and light availability.

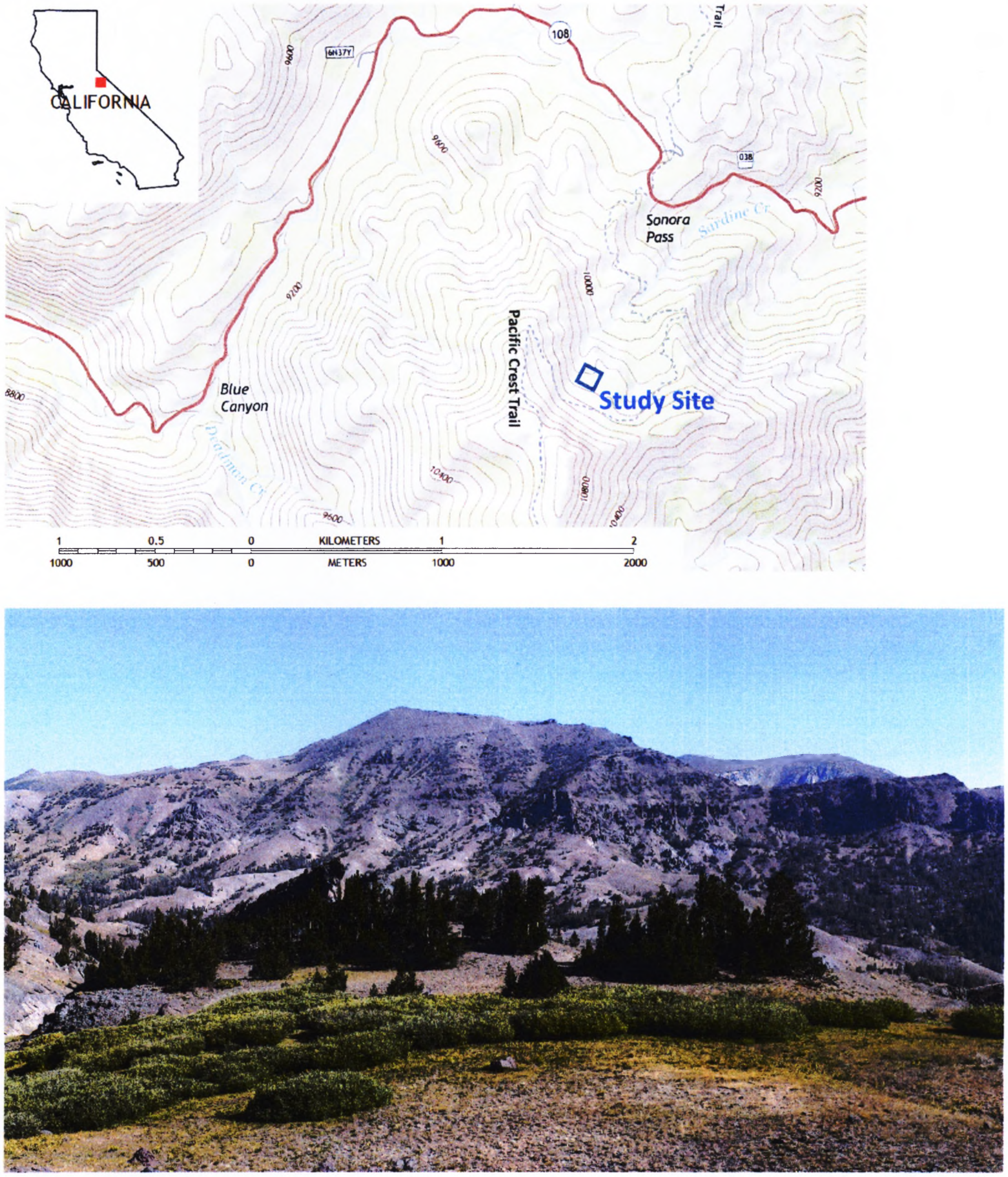

Figure 1. Site map and photo. (a) Topographic map of study site and region (elevation units in feet, with 80 ft. increments); inset map shows location of Sonora Pass in the Central Sierra Nevada range in California (USGS, 2015). **(b)** Photo of study site as viewed from Pacific Crest Trail looking north.

2.2. Quantifying Inter-tree Competition

Inter-tree competition is defined as the collective competitive stress from neighbor trees to a focal tree and typically expressed as an index (CI). A number of ways exists in general forestry practices to quantify inter-tree competition; they largely fall under two large categories: distance-independent (Glover and Hool, 1979; Lorimer, 1983) and distance-dependent (Hegyi, 1974; Canham et al., 2004). Distance-independent CI generally perform well in relatively even-aged, even-distributed forests and plantations (Lorimer, 1983). However, more complex, distance-dependent CI may be needed in structurally-diverse environments (Aakala et al., 2013). We elect to use a size and distance-dependent CI in the middle of the complexity spectrum (Aakala et al., 2013) to quantify inter-tree competition at our treeline site (Eq. 2; modeled after Hegyi, 1974).

Equation 2

$$CI_F = \sum_{i=1}^{n} \frac{Size_i}{Size_F} \times \frac{1}{Distance_{Fi}}$$

Our competition index of a focal tree (CI_F) is directly proportional to the ratio of the neighboring tree size ($Size_i$) relative to the focal tree size ($Size_F$), factoring in the sensitivity of the focal tree to neighbors based on the size of the focal tree itself – smaller trees are more sensitive to neighbor influence than larger trees. $\mathrm{CI_F}$ is also inversely related to the distance to neighboring trees ($Distance_{Fi}$); farther neighbors exert less competition to the focal tree. Lastly, $\mathrm{CI_F}$ sums over all neighboring trees (n) within a critical radius. This index provides a useful surrogate to determine a tree's access to resources such as light, water, or nutrients in the presence of neighbors, and we use it as an independent variable to test for influence of small-scale environmental variations on tree growth.

To obtain the parameters discussed above, we set up circular plots across the field site and mapped the position and size of every tree having a diameter at breast height (DBH) greater than 10cm. Nine plots were established to cover 217 trees mapped. Each circular plot has a center base (Fig. 2) and includes trees within a radius of about 25m (instrument limitation); the number of trees in each plot vary depending on the density of the area covered. We measured the distance of each tree within the plot to the center using a vertex instrument (Haglöf Vertex IV), which communicates sonically between a transponder placed at tree and a receiver place at the base. That is coupled with a Brunton compass to measure the azimuth angle of each tree to the center point to establish tree positions using polar coordinates. These measurements were later converted to x-y coordinates to calculate tree-to-tree distances and directions; they are also referenced to B3 (Fig. 2), a central point for study site for further calculations.

We quantify tree size as $(1/3)*h*r^2$, which corresponds to trunk volume for a cone with height h and breast height-radius r. Hegyi's original CI calculation used DBH to represent tree size, we chose trunk volume over DBH because there is large variabilities in tree shape. Taking into account both the girth and height of the trees offers a more comprehensive representation of the effect of size on competition. (Competition calculations using DBH alone as size estimator produce similar distributions as trunk volume. Results of this study using DBH are included in the Appendix.) The critical radius determines the horizontal spatial extent of neighborhood competition and affects of number of neighborhood trees included in the CI calculation. We applied a conservative critical radius of 20m, which is approximately twice the vertical height of the tallest trees at the study site.

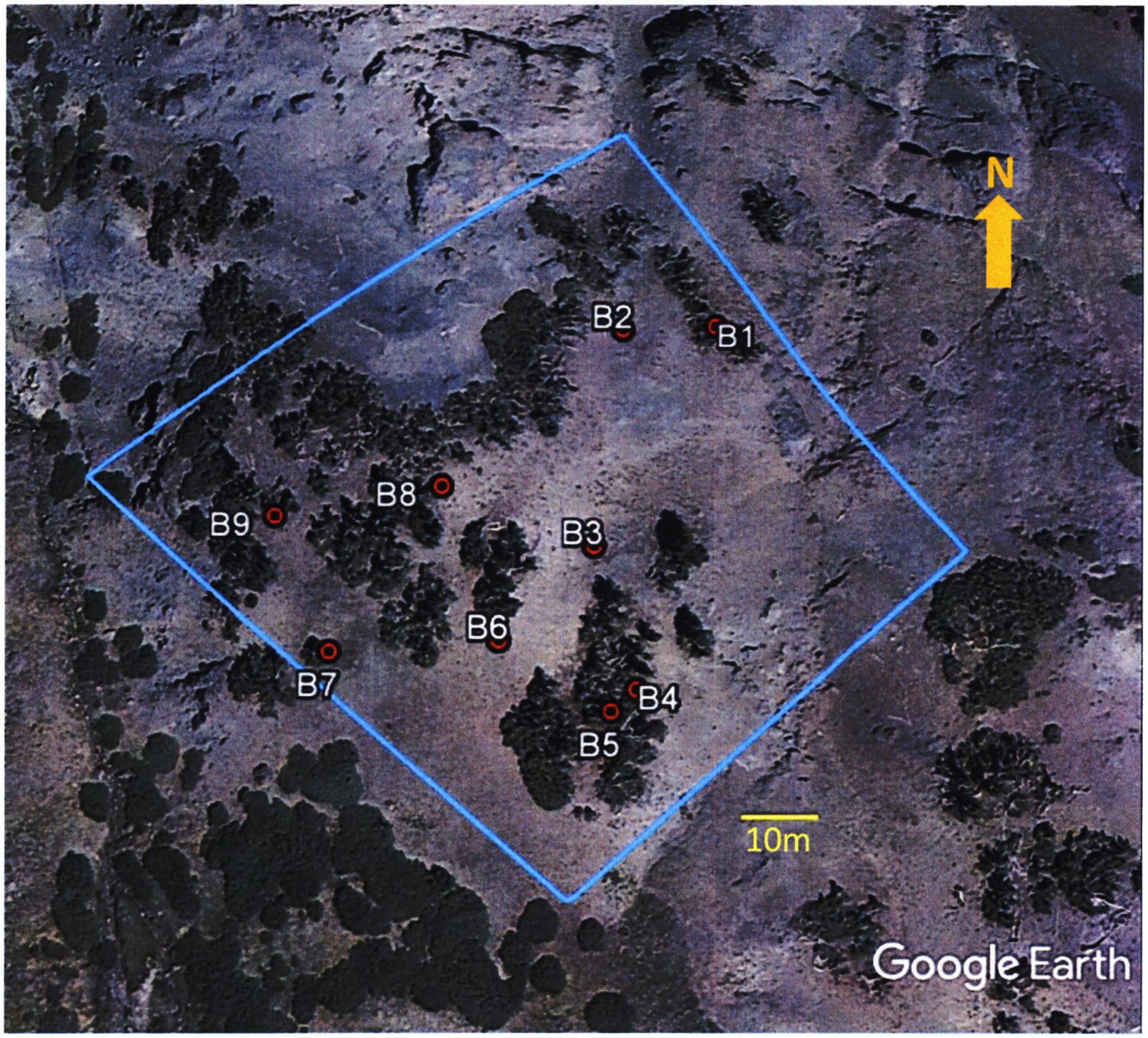

Figure 2. Circular survey plots. Location of nine bases overlaid on Google Earth

2.3. Quantifying Mean Growth Rate

We cored each tree with DBH greater than 12cm and averaged the tree ring widths (TRW) over the most recent 20 years (1995-2014) as a surrogate for annual growth. A total of 178 trees were sampled, with two cores per tree removed and processed following standard dendrochronology practices (Stoke and Smiley, 1968). Ring width measurements from two cores of one tree were averaged to represent growth for that tree. Previous studies on competition-growth relationships have used basal area increment (BAI) instead of average ring width to represent growth (e.g. Aakala et al, 2013). However, BAI is a dangerous metric because it is a function of DBH of the focal tree, a variable that appears in the denominator of CI (Eq. 2). To avoid this potential bias, we take the mean TRW over the last 20 years as our index of growth. This represents a balance between choosing an appropriate threshold period assuming consistent growth under the observed environment and choosing a long enough period to minimize the year-to-year ring width variabilities. Adopting a BAI approach leads to qualitatively identical results, except in that the correlations are quantitatively much stronger. To minimize age-related growth effects from young trees, tree younger than 50 years of age were excluded.

3 RESULTS

3.1 Competition Negatively Modulates Growth

We find that the logarithm of growth rate is significantly correlated with the log of our index of inter-tree competition ($r = -0.46$, $p < 0.001$; Fig. 3). The negative relationship between these two quantities implies that competition limits tree growth in our treeline environment. This correlation remains unchanged ($r = -0.46$, $p < 0.001$; Fig. 3) when we removed 13 outliers having a Cook's distance greater than three times the mean Cook's D, indicating that the outliers have relatively similar magnitude but opposite direction of leverage. Most of the outliers that over-predicts growth rate (Trees numbered 109, 110, 170, 178, and 171) display growth releases in recent decades. It is unclear whether these releases are associated with (reduced) competition or other mechanisms. There is less common patterns about the outliers that under-predict growth. Tree #66 has a large DBH of 48.8cm, however, the main trunk is split open and the center is hollow. The split may have artificially overestimated the size of the tree and consequently underestimated the CI. We also noted the presence of small trees and bushes on some of the edges of the site. Because they were not quantified to be included in the competition calculations, it is possible that the CI for trees near these bushes were underestimated.

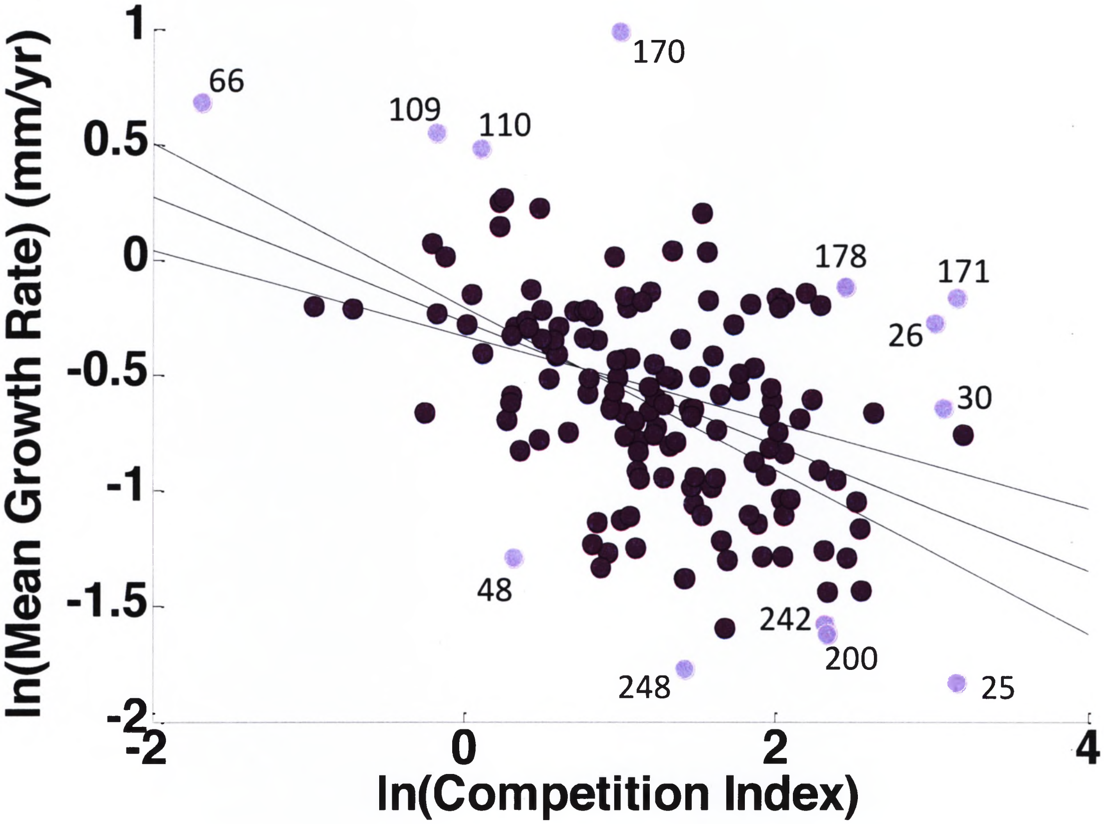

Figure 3. Relationship between growth rate and competition. Competition index (x-axis) versus the mean growth rate, calculated as the average growth over the last 20 years for each core (y-axis). The two series are significantly negatively correlated on a log-log scale ($r = -0.46$, $P < 0.001$). The solid black line indicates the best least-squared log-log fit, and the dotted lines indicate the 95% uncertainty of log-log slope. Outliers (data points having Cook's distance greater than three times the mean Cook's D) are highlighted in light purple and labelled with tree ID.

3.2 Moisture Signal Not Detected

It has been demonstrated that growth at the Sierra Nevada treeline responds positively to precipitation (Stephenson, 1990). To identify the imprint of competition for water availability, we compared the competition-growth relationship between wet and dry years under the hypothesis that the relationship would be stronger during dry years if the trees are competing over water availability. Instead of averaging all 20 years of TRW to calculate mean growth rate, we divided the TRW into two 10-year groups based on March through October (assumed growing season) accumulated precipitation from the nearby Deadman Creek weather station (38.33°, -119.65°, 2819m). The wetter half corresponds to years 1995, 1996, 1998, 1999, 2005-2007, 2010, 2011, and 2014, whereas the drier half corresponds to years 1997, 2000-2004, 2008, 2009, 2012, and 2013. The competition signal accounting for only the wetter half and only the drier half of growth are visually similar (Fig 4a and 4b), which suggests that moisture availability may not be a dominant control on competition at our treeline site. If absolute growth rate differences among the trees are large compared to inter-annual growth variability then the signature of competition for water may be obscured. In order to isolate effects of inter-annual moisture variability, we further compared competition index with the ratio of growth during dry years to that of wet years (Fig 4c). The lack of relationship again demonstrates that competition for moisture does not appear to be a dominant control of difference in growth rates.

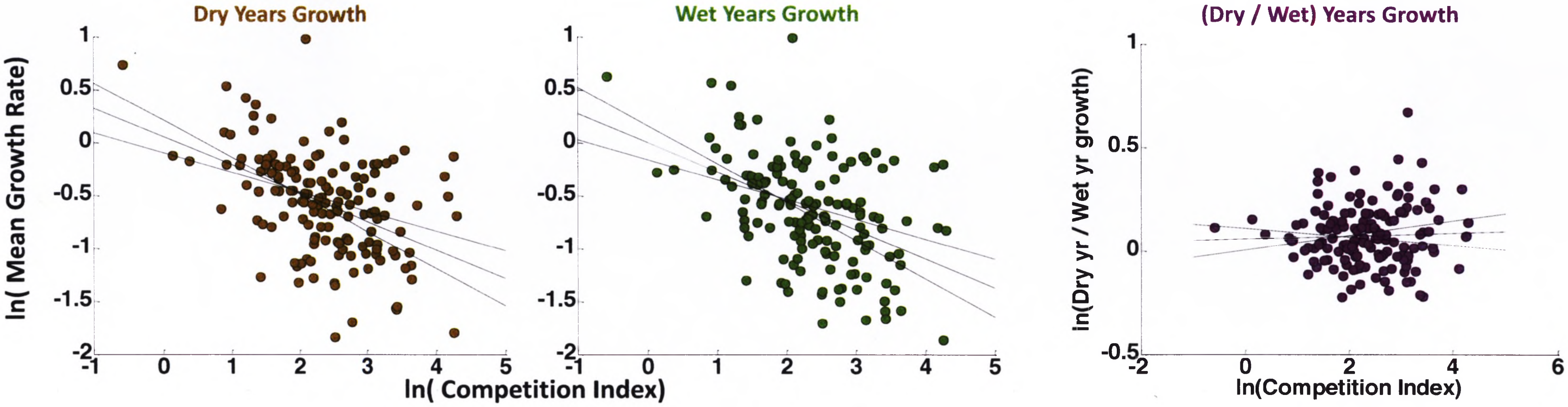

Figure 4. Competition-growth relationship for dry and wet years. Axes similar to Fig 3. **(a)** Growth rate calculated using the drier half of the last 20 years ($r^2 = 0.21$, $p < 0.01$); (b) using the wetter half of the last 20 years ($r^2 = 0.21$, $p < 0.01$); (c) and using ratio of drier to wetter years ($r^2 = 0.00$, $p = 0.61$). Solid lines indicate the slopes of the relationship; dashed lines indicate the 95% confidence interval estimate about the slope.

3.3 Competition for Incident Radiation

The argument of light limitation at treeline is generally rejected, citing that trees would not be competing for sunlight in an open-canopy environment. However, as we observe from the actual field environment (Fig 1b), trees do tend to cluster and create shading over their neighbors. The Vaganov-Shashkin model (Eq. 1) also indicates that growth having a directly response to sunlight availability. To test for influence of solar radiation interception, we selectively weighed neighborhood trees in the CI calculations under two scenarios: by treetop height and by direction.

Typically, taller trees have the advantage in intercepting direct solar radiation and shade their shorter neighbors. A focal tree would experience greater light competition from neighbor trees with higher treetop height (ground elevation plus tree height) than from neighbors with lower treetops. We tested this hypothesis by comparing the competition signals from two groups of neighbor trees: those that have higher treetop heights than the focal and those with lower treetop heights. The competition-growth relationship is pronounced and significant when only trees with higher treetop heights are included (Fig 5a, $r = -0.43$, $p < 0.01$). However, no significant relationship exists in the case that only considers lower treetop neighbors (Fig 5b, $r = -0.10$, $p = 0.27$). This is consistent with our hypothesis that differences in mean growth rates are driven by differential access to solar radiation, with taller trees shading shorter ones.

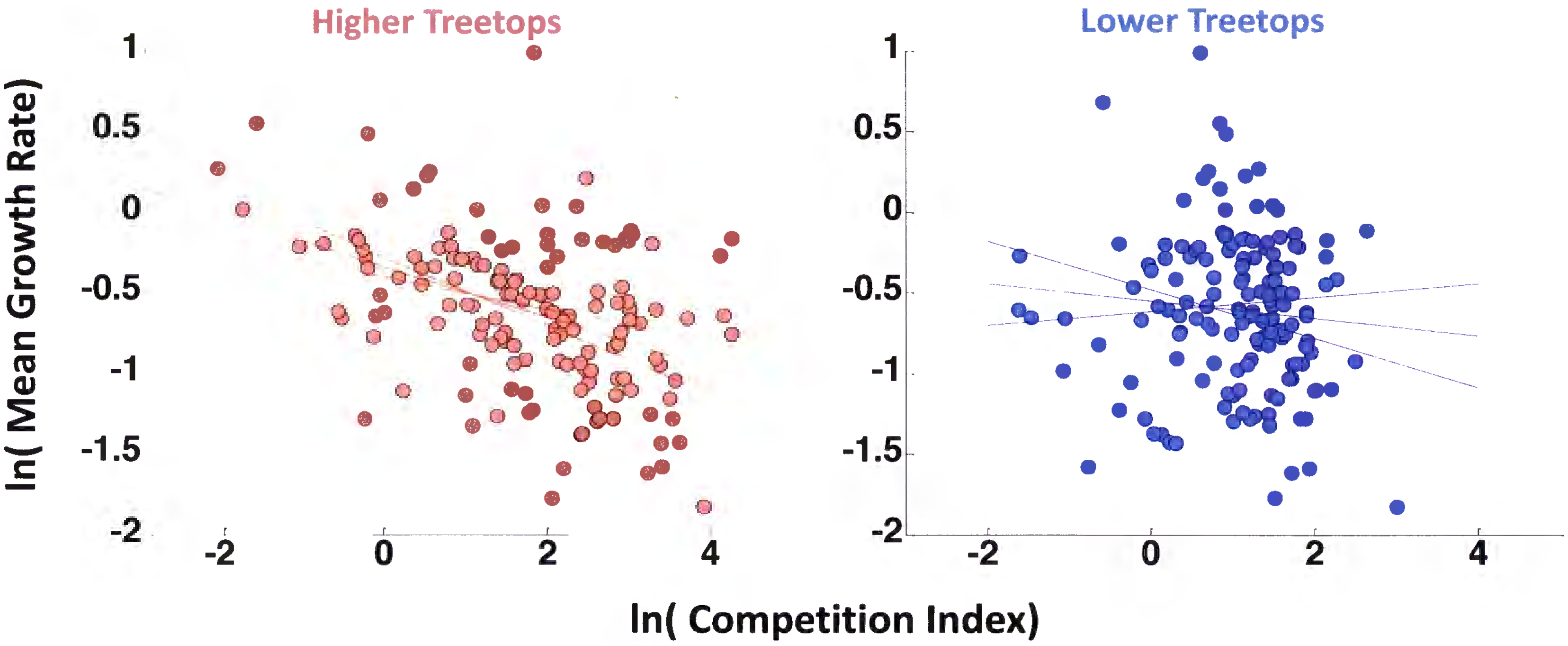

Figure 5. Competition-growth relationships by neighbor treetop heights. Axes similar to Fig 3. Competition indices are integrated over neighbor trees with higher **(a)** and lower **(b)** treetop heights than focal tree. Competition-growth relationship is negative and significant in the presence of taller trees ($r = -0.43$, $p < 0.01$) but not of shorter trees ($r = -0.10$, $p = 0.27$).

Incident radiation also vary by direction, providing another test to compare the effects of competition on growth differed by locations of neighbor trees. We modified the CI calculations by grouping neighbor trees into north and south of focal tree and reconstructed the competition-growth relationships for each. When only neighbor trees to the south are included, the competition signal is negative and significant (Fig 6a, $r = -0.43$, $p < 0.01$), whereas when only neighbor trees to the north are included the relationship is relatively weak and scattered (Fig 6b, $r = -0.24$, $p < 0.01$). These observations suggest that competition from neighbor trees to the south, where more direct sunlight is available, exerts greater growth stress than that from neighbor trees to the north, which is again consistent with the hypothesis that growth is influenced by sunlight availability.

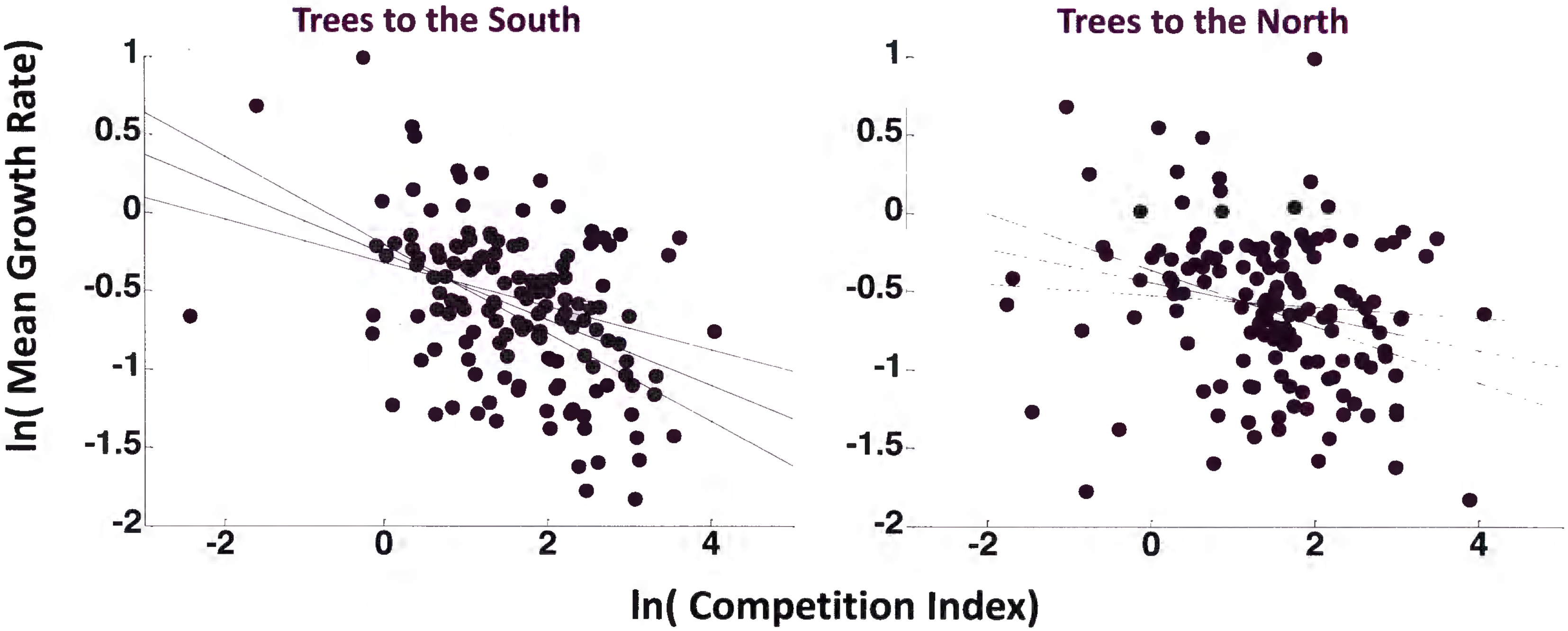

Figure 6. Competition-growth relationships by direction. Axes similar to Fig 3. Competition indices are integrated over area south (left plot) and north (right plot) of focal tree. Competition-growth relationship is negative and significant from neighbor trees to the south ($r = -0.43$, $p < 0.01$) but weaker from trees to the north ($r = -0.24$, $p < 0.01$).

The previous method of estimating light competition by direction is equivalent to assigning binary weights of 1 or 0 to neighbor trees based on position to north or south of the focal tree. This method gives equal weights to neighbor trees located directly south (or north) of the focal tree as to those located primarily to the east or west but are merely south (or north) of the focal tree. However, this binary differentiation is not a natural way to describe incident radiation because direct sunlight reaches the top of the canopy over a continuous spectrum of directions at varying intensity. Neighbor trees would cast different amounts of shading to the focal tree depending on their azimuth angle to the focal tree. We model this angle-dependent weight using a von Mises function (Equation 3) so that neighboring trees located in a certain direction of interest are weighed more than trees located away from that direction. The von Mises weight (Equation 4) of each neighbor tree (vM_i) is a function of the azimuth angle of the neighbor tree (θ_i) to the focal tree relative to the direction of interest (μ). Instead of using 1 and 0 to indicate north or south, all trees within the critical radius are included in the CI calculation, with trees located closer to the direction of interest (θ_i approaches μ) being weighed more than trees away from that direction. The K value is a scaling factor that modifies the width of the function; we applied $K = 2$ for this analysis to favor weighing in the direction of interest without compromising potential competition stresses from trees in other directions. By looping the direction of interest (μ) from $-\pi$ to π, we constructed competition-growth relationships for all increments of directions and computed the coefficients of determination (r^2) to represent the strength of the relationship for each.

Equation 2

$$CI_F = \sum_{i=1}^{n} \left(\frac{Size_i}{Size_F} \times \frac{1}{Distance_{Fi}} \times vM_i \right)$$

Equation 3

$$vM = \frac{e^{K \times \cos(\theta_i - \mu)}}{2\pi}$$

We find again that the strongest correlations in the southern directions and nearly non-existent from the north. That is, competition from neighbor trees to the south exerts more growth stress on the focal tree than neighbor trees to the north (Fig 7a, purple line).

When accounting for only trees with higher treetops, the resulting correlations hold a similar shape (Fig 7b, pink line), suggesting that treetop height is important for competition but sunlight direction also plays an important role. When accounting for only trees with lower treetops (Fig 7b, blue line), there are no correlations between competition and growth in any directions, which is consistent with our understanding that trees with lower treetop height than the focal tree do not exert light competition on the focal tree.

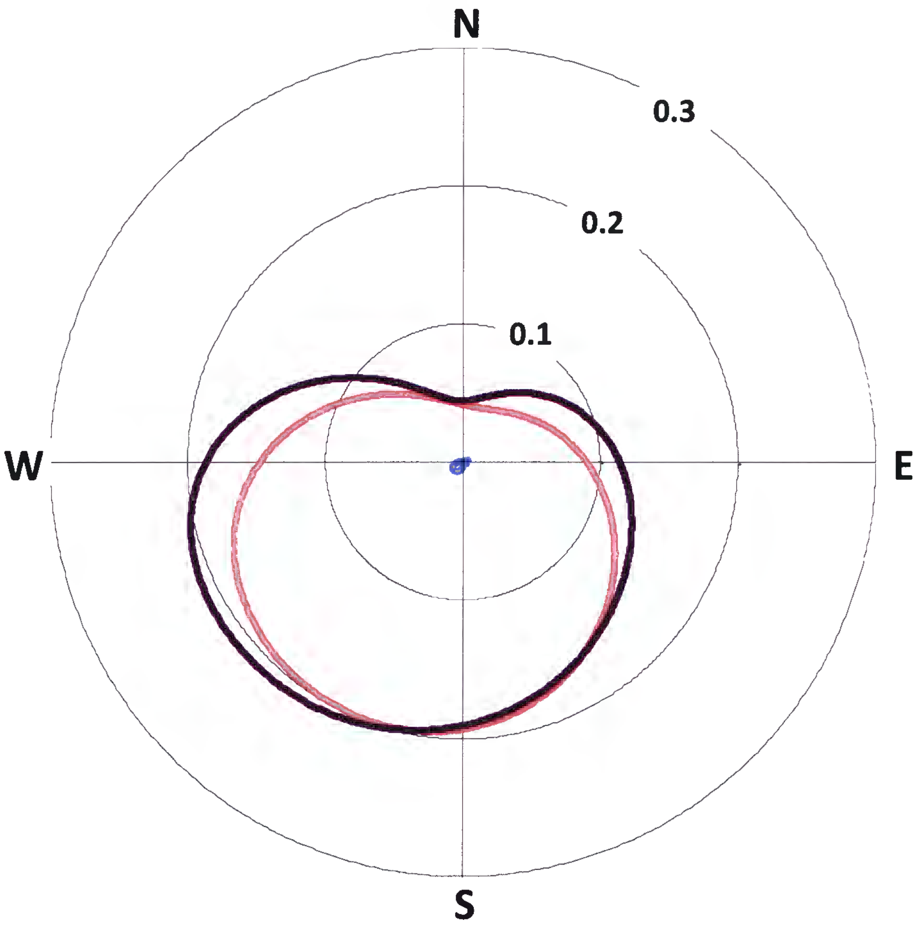

Figure 7. Competition controls mean growth where light is available. From Figures 4c and 4d, integrate competition over all directions and weigh trees with a von Mises distribution for each direction; radii of circles indicate the r^2 values. Competition includes all neighbor trees (grey, significant), only neighbors with higher treetop elevation (red, significant), and only neighbors with lower tree-top elevation (blue, not significant).

4 DISCUSSION

4.1 Tree Unlikely to be Competing for Water

The lack of a clear moisture signature in the competition-growth analysis may be a surprise to other studies in the Sierra treeline, which suggested water availability as an important control on growth (Stephenson, 1990). Water availability at our study site may be unimportant on growth for several reasons. The treeline ecotone in this region spans a large vertical zone rather a narrow band. Low-statue trees and krummholz formations are found as low as 100 meters below our field site on wind-exposed ridges, and upright standing trees of at least 3m continue for another approximately 20 meters above our site, albeit on steep slopes that are difficult to access. Trees growing across a vertically extensive treeline zone in the Sierras may be sensitive to different climate variables, with upper treeline growth more responsive to temperature variabilities but lower treeline growth correlating more with precipitation (Salzer et al., 2014). Instead of sampling from steep gradients as in a number of studies (e.g. Graumlich, 1993), we selected a relatively flat area to maximize a consistent horizontal distribution of water. The presence of a wet meadow adjacent to our site and a seasonal stream that flows through the site at least through July suggest that moisture is unlikely to be limited. Lastly, there are potential interactions between variables. Warmer and wetter conditions combined promote growth, whereas warmer or wetter alone do not contribute to significant growth promotion (Bunn et al., 2005).

4.2 Possible Mechanisms for Incident Radiation Competition

Our results demonstrated that growth at treeline is affected by differential access to incident solar radiation. However, because of strong correlations between sunlight availability and heat, the interpretation of the growth driver is less clear. While light provides the direct energy necessary to initiate the photosynthesis mechanism, heating at the leaf and ground level also create a favorable environment for carbon assimilation. We consider three mechanistic explanations of our results.

4.2.1 Leaf Temperature

Shading between trees creates competition for environmental temperature. Trees under direct sunlight are warmed more readily at the leaf level and have access to favorable growing conditions than trees in the shade, which may experience lower leaf temperature that limits growth. However, the range of ambient temperature experienced in the growing season makes this argument implausible. In the low temperature range, stomatal conductance increases with temperature but only shuts down if temperature drops below a critical threshold. Over two summers of field campaign, daytime temperature at the site was uncomfortably warm for work. Deadman Creek (DDM) weather station located 311m below the field site recorded average maximum May-Oct temperature to be 15.8°C (ranging from 10.4°C in May to 20.5°C in July), suggesting that tree growth under shade would not be temperature limited. Stomatal conductance is also maximized at optimal temperatures that aligns with the mid-late morning period. This is a balance between achieving warm enough temperatures for carbon fixation but not too warm (afternoon) where the stomata experience moisture stress and begin to close. Mid-morning sun casts light from the southeast, inconsistent with our results which do not indicate a strong asymmetry between the southeast and southwest directions.

4.2.2 Soil Temperature

One of the most widely accepted models on treeline height points to soil temperature as a key control (Korner and Paulsen, 2004). If the competition signal is tied to warmer soil temperature alone, then shading on the ground from neighbors would produce similar effects regardless of the size of the focal tree. This is distinct from the light competition hypothesis where interception of solar radiation scales with focal tree size. We propose a test to differentiate the two potential mechanisms by defining new CI's where the term of focal tree size ($1/S_F$) is excluded. If the competition-growth relationship remains significant using the new CI's, then soil temperature could be a potential candidate for controlling the growth differences between trees.

Differential heating of soil may also cause temporal lag in response. Trees with low competition have small or far away neighbors, exposing them to direct sun sooner in the growing season. Thus the inter-annual growth patterns of low-CI trees are more likely to correlate with early summer temperature (i.e. June) than those of high-CI trees. In conjunction with the chronology development work discussed in Chapter 1, we propose another test to relate CI and ring-width correlations with monthly temperatures. If the growth of trees at our field site are in competition for soil temperature, the low-CI trees would produce ring width patterns correlated with most of the growing season monthly temperatures (presumed Jun-Sep), whereas high-CI trees would correlate less with early season temperature (Jun) but more with late season temperature (July-Sep).

4.2.3 PAR Sensitivity

Sun leaves are able to achieve higher assimilation rates than shade leaves when irradiance is high. Across the central Sierras, summer growing season is generally warm and clear, providing abundant light for trees that have access and contrasting with those without access. Our results are consistent with this light competition hypothesis – higher growth rate is associated with less competition (Fig 2). Low competition refers to trees that are larger than their neighbors or have fewer neighbors, and they are likely to have more access to direct sunlight.

The behaviors of the quantum yield curves between sun and shade leaves at low irradiance offers important clues to understand growth response in a reduced light environment. Under ideal conditions (no temperature and moisture stress and no CO2 limitation), the initial quantum yields are shown to be similar for sun and shade leaves (Bjorkman, 1981; Ogren, 1993), although shade leaves tend to have a lower light compensation point (Bjorkman, 1981; Ogren, 1993), giving to higher assimilation rates at low light than sun leaves. However, a treeline environment may complicate such response. Large-scale light limitation analyses showed that treeline growth in cool and cloudy regions are more sensitive to light reduction than those in warm and clear regions (Stine and Huybers, 2014). To test this, we propose to measure assimilation rates from trees at two ends of the competition index spectrum and under various irradiance levels.

Our experiment which is based on tree-level variabilities of sun and shade can be extrapolated to large-scale tree growth in clear and cloudy regions, respectively. The quantum yield curves at low irradiance levels simulate growth response at a reduced-light environment such as post-volcanic eruptions or global dimming. According to the findings by Stine and Huybers (2014) and Tingley et al. (2014), we would expect shade leaves (high CI) to yield less growth than sun leaves.

4.3 Ghost Competition

Given the observation of competition-influenced tree growth, it is tempting to take the variability in growth explained by competition and apply that to the full tree-ring width time series. However, forests are dynamic and the competition environment evolves over time. We cannot directly observe or measure competition in past years, a concept termed as ghost competition. The effects of ghost competition is amplified in forest of rapid growth and fast-turnover rates but relatively small in slow-growth, temperature-stressed treeline environment like our field site. Nevertheless, it can be dangerous to treat inter-tree competition consistent in temporal growth variability analysis because there is no predictor function to model ghost competition. The past environment could have been more competitive (e.g. more neighbors present but some died and fell down later) or less (e.g. some neighbors had not established or grown up yet) or simply different. While there may not be systematic bias in the correlation between the current competition and temporal variability of tree-ring width, the correlations, if any, also do not reflect meaningful relationships.

Several methods exist to quantify ghost competition and to identify its influence on climate reconstructions using tree-ring records. Dead logs on the ground can be cored and cross-dated with the chronology developed using living trees to determine when the fallen trees died. Their size and location can also be measured to estimate the ghost competition index. This method has been demonstrated in structurally-even eastern forests for stand dynamic studies (Aakala et al., 2013). It also works well at treeline for extension of climate reconstructions because of slow decay rates and a relatively undisturbed environment. However, it may be challenging at our field site because of its close proximity to the highly used Pacific Crest Trail and clear signs of campfires at the site. A less direct method to measure ghost competition is to detect growth suppressions and releases in the ring width series. Growth suppressions and releases are associated with rapid changes in stand structure and usually recorded as sudden switches between a series of wide rings and a group of narrow rings. By linking the pattern and timing of the suppression and release events and the locations of the trees, this method remaps the competition environment of the past.

4.4 New Growth Model for Treeline Trees

Since we have identified a strong relationship between competition index and growth rate, we can establish a new tree growth model as a function of competition as well as biological age effect and climate variabilities. (Eq. 5).

Equation 5 $$TRW_F = (b \times {CI_F}^{-a}) \times (d \times {Age_F}^{-c}) \times Climate + noise$$

The tree-ring width variability for each focal tree (TRW_F) over time is predicted by the competition (*CI*) experienced by the focal tree, age of the tree, overall climate controls of the environment, and random variabilities (*noise*). Competition and growth rate are inversely related on a log-log scale, thus both the CI and Age terms are written as negative exponential functions with intercepts *b* and *d* and slopes *a* and *c*, respectively. However, competition and age are not independent of each other (Eq. 6).

Equation 6 $$b \times {CI_F}^{-a} = b \times \left(\sum_{i=1}^{n} \frac{Size_F}{Size_i} \times Distance_{Fi} \right)^{a}$$

By definition of our CI in Eq. 2, the sizes of the focal tree and the neighbor trees are functions of time (age), and younger trees tend to be more sensitive to competition than older trees. When fitting an age curve to a tree-ring series, as is commonly done in TRW-climate analyses and demonstrated in Chapter 1, the curve generally contains not only the true age effect but also some low-frequency variabilities from climate and potentially from the evolving competition environment (Eq. 7).

Equation 7 $$AgeCurve_{Fit} = AgeCurve_{True} \times \mathcal{F}_{LP}(CI) \times \mathcal{F}_{LP}(Climate)$$

$\mathcal{F}_{\mathrm{LP}}$ indicates a low-pass filter for competition and climate variabilities. The loss of low-frequency climate signal in the standardization process is known as the "segment length curse" (Cook et al. 1995). The case we have presented in Eq. 7 is more problematic. Even if we could identify the true age effect ($AgeCurve_{True}$), the remaining term contains both low-frequency inter-tree competition and climate information that are not easily separated.

A similar problem exists at the high frequencies but it may be resolvable. The process of removing the age-related trend in the TRW series to recover the climate signal is achieved by dividing Eq. 5 by Eq. 7 above (Eq. 8).

Equation 8 $$Climate_{Fit} = \mathcal{F}_{HP}(CI) \times \mathcal{F}_{HP}(Climate) + noise$$

$\mathcal{F}_{HP}$ indicates a high-pass filter for competition and climate variabilities. $Climate_{Fit}$ is the residual time series after standardization, and it is conventionally interpreted as the climate variability in tree-rings. However, as in the low-frequency case, the climate signal is now masked by the additional competition term. The good news is – we may be able to detect the high-frequency competition signal over time. Section 2 of this study demonstrates how to quantify inter-tree competition for the current environment, and Section 4.3 discusses methods to reconstruct pulses of ghost competition using cross-dating of dead logs and growth suppression / release patterns in the TRW record. Detecting $\mathcal{F}_{HP}(CI)$ provides us an opportunity to improve the climate signal-to-noise ratio extracted from the TRW record.

4.5 Implications for Light and Temperature Reconstructions

The effect of inter-tree competition at a treeline environment may have been viewed in the past as part of the noise in the tree-ring records. Our results provides a case for the presence of competition-influenced growth and suggests that this competition is likely tied to availability of incident solar radiation. Furthermore, the possibility of detecting a temporal signal of competition offers two important opportunities for understanding tree ring records sampled from treelines. First, because instrumental light records are very sparse temporally and spatially, it may be possible to reconstruct light availability time-series using existing and future tree-ring collections. Second, light competition may affect the ring record's sensitivity to temperature variability at the tree level. Normal sampling method for temperature-reconstruction focuses on isolated trees to avoid the effects of competition. By demonstrating a relationship between competition and temperature, we may gain insights on how to select trees to improve the temperature signal in the tree-ring record.

5 CONCLUSION

This study combines two well-studied dendrochronology practices: developing a ring-width chronology from treeline to reconstruct temporal climate variability and quantifying inter-tree competition to reconstruct spatial stand dynamics. While our TRW record collected near Sonora Pass, CA largely reflects early summer temperature as growth control, the presence of a significant competition-growth relationship demonstrates another important mechanism limiting growth at treeline. Moreover, this competition favors the directions of incident solar radiation, i.e. stronger and more significant when accounting for competition from neighbor trees to the south, as opposed to north, and neighbor trees with a higher treetop height, as opposed to those with lower treetops. These results support the hypothesis that selection of trees for temperature reconstruction is also limited by competition where is tied to the effects of light, and they contribute to a new understanding of the physical processes controlling growth at treeline. Our findings provides a roadmap for further research on past competition environments and on investigating the relationship between the competitions a tree experiences and its temporal sensitivity to temperature variability. These relationships complicate our previous interpretations of treeline TRW chronologies used for temperature reconstruction, but they offer opportunities to fine-tune temperature estimates during radiation-limited periods. They also provide important clues on tree selection in future collections and reconstructions to maximize the desire climate signal.

6 REFERENCE

Aakala, T., Fraver, S., D'Amato, A. W., & Palik, B. J. (2013). Influence of competition and age on tree growth in structurally complex old-growth forests in northern Minnesota, USA. Forest Ecology and Management, 308, 128-135.

Bjorkman, O. L. L. E. (1981). response of photosynthesis to temperatures. In Symposium-British Ecological Society.

Briffa, K. R., P. D. Jones, and F. H. Schweingruber (1992), Tree-Ring Density Reconstructions of Summer Temperature Patterns across Western North America since 1600, J. Climate, 5(7), 735–754, doi:10.1175/1520-0442(1992)005<0735:TRDROS>2.0.CO;2.

Bunn, A. G., L. J. Graumlich, and D. L. Urban (2005), Trends in twentieth-century tree growth at high elevations in the Sierra Nevada and White Mountains, USA, The Holocene, 15(4), 481–488, doi:10.1191/0959683605hl827rp.

Canham, C. D., LePage, P. T., & Coates, K. D. (2004). A neighborhood analysis of canopy tree competition: effects of shading versus crowding. Canadian Journal of Forest Research, 34(4), 778-787.

Cook, E. R., Briffa, K. R., Meko, D. M., Graybill, D. A., & Funkhouser, G. (1995). The'segment length curse'in long tree-ring chronology development for palaeoclimatic studies. The Holocene, 5(2), 229-237.

Glover, G. R., & Hool, J. N. (1979). A basal area ratio predictor of loblolly pine plantation mortality. Forest Science, 25(2), 275-282.

Graumlich, L. J. (1993), A 1000-Year Record of Temperature and Precipitation in the Sierra Nevada, Quaternary Research, 39(2), 249–255, doi:10.1006/qres.1993.1029.

Hadley, J.L. & Smith, W.K. (1990) Influence of leaf surface wax and leaf area to water content ratio on cuticular transpiration in western conifers, USA. Canadian Journal of Forest Research, 20, 1306–1311.

Harsch, M. A., & Bader, M. Y. (2011). Treeline form–a potential key to understanding treeline dynamics. Global Ecology and Biogeography, 20(4), 582-596.

Hegyi, F., 1947. A simulation model for managing jack-pine stands. Growth models for tree and stand simulation. (30) pp. 74–90.

Hoch, G. & Körner, C. (2009) Growth and carbon relations of tree line forming conifers at constant vs. variable low temperatures. Journal of Ecology, 97, 57–66.

Holtmeier, F. (2009) Mountain timberlines: ecology, patchiness, and dynamics, 2nd edn Springer, New York.

Holtmeier, F. & Broll, G. (2005) Sensitivity and response of Northern Hemisphere altitudinal and polar treelines to environmental change at landscape and local scales. Global Ecology and Biogeography, 14, 395–410.

Körner, C. & Paulsen, J. (2004) A world-wide study of high altitude treeline temperatures. Journal of Biogeography, 31,
713–732.

Lorimer, C. G. (1983). Tests of age-independent competition indices for individual trees in natural hardwood stands. Forest Ecology and Management, 6(4), 343-360.

Malanson GP. 1997. Effects of feedbacks and seed rain on ecotone patterns. Landscape Ecology 12:27–38.

Ögren, E., & Evans, J. R. (1993). Photosynthetic light-response curves Planta,189(2), 182-190.

Pereg, D. & Payette, S. (1998) Development of black spruce growth forms at treeline. Plant Ecology, 138, 137–147.

Salzer, M. W., E. R. Larson, A. G. Bunn, and M. K. Hughes (2014), Changing climate response in near-treeline bristlecone pine with elevation and aspect, Environ. Res. Lett., 9(11), 114007, doi:10.1088/1748-9326/9/11/114007.

Schweingruber, F. and Briffa, K.Tree-Ring Density Networks for Climate Reconstruction, Climate Variations and Forcing Mechanisms of the Last 2000 Years, 43-66 (Springer, 1996).

Stephenson, N. L. (1990). Climatic control of vegetation distribution: the role of the water balance. The American Naturalist, 135(5), 649-670.

Stine, A. R., and P. Huybers (2014), Arctic tree rings as recorders of variations in light availability, Nat Commun, 5(3836), doi:10.1038/ncomms4836.

Stokes, M. A., and T. L. Smiley. 1968. An introduction to tree-ring dating. University of Chicago Press, Chicago, Illinois, USA.

Tingley, M., A.R. Stine, and P. Huybers (2014), Temperature reconstructions from tree-ring densities overestimate volcanic cooling, Geophysical Research Letters, v41(22), p7838-7845, 2014

Tranquillini,W. (1979) Physiological ecology of the alpine timberline. Springer-Verlag, New York.

Vaganov, E. A., M. K. Hughes, and A. V. Shashkin (2006), Growth Dynamics of Conifer Tree Rings, Ecological Studies, Springer-Verlag, Berlin/Heidelberg.